BIOMINERALIZATION OF HYDROXYETHYL CELLULOSE/SODIUM ALGINATE IMPREGNATED WITH CELLULOSE NANOCRYSTALS BY USING SURFACE MODIFICATION TECHNIQUE

ETDAL BAKHIET

MASTER OF SCIENCE

UNIVERSITI MALAYSIA PAHANG

UNIVERSITI MALAYSIA PAHANG

DECLARATION OF THESIS AND COPYRIGHT

Author's Full Name : ETDAL BAKHIET

Date of Birth : 14 MAY 1964

Title : BIOMINERALIZATION OF HYDROXYETHYL CELLULOSE/SODIUM ALGINATE IMPREGNATED WITH CELLULOSE NANOCRYSTALS BY USING SURFACE MODIFICATION TECHNIQUE

Academic Session : SEMESTER 1 2020/2021

I declare that this thesis is classified as:

☐ CONFIDENTIAL (Contains confidential information under the Official Secret Act 1997)*

☐ RESTRICTED (Contains restricted information as specified by the organization where research was done)*

☑ OPEN ACCESS I agree that my thesis to be published as online open access (Full Text)

I acknowledge that Universiti Malaysia Pahang reserves the following rights:

1. The Thesis is the Property of Universiti Malaysia Pahang
2. The Library of Universiti Malaysia Pahang has the right to make copies of the thesis for the purpose of research only.
3. The Library has the right to make copies of the thesis for academic exchange.

Certified by:

_____
(Student's Signature)

563132139
_____
New IC/Passport Number
Date:

_____
(Supervisor's Signature)

Dr Farah Hanani Zulkifli
_____
Name of Supervisor
Date:

NOTE : * If the thesis is CONFIDENTIAL or RESTRICTED, please attach a thesis declaration letter.

SUPERVISOR'S DECLARATION

I hereby declare that I have checked this thesis and in my opinion, this thesis is adequate in terms of scope and quality for the award of the degree of Master of Science.

_____

(Supervisor's Signature)

Full Name   : DR FARAH HANANI ZULKIFLI

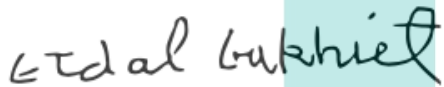Position   : SENIOR LECTURER

Date   : JANUARY 2021

STUDENT'S DECLARATION

I hereby declare that the work in this thesis is based on my original work except for quotations and citations which have been duly acknowledged. I also declare that it has not been previously or concurrently submitted for any other degree at Universiti Malaysia Pahang or any other institutions.

Etdal Bakhiet

_____

(Student's Signature)

Full Name   : ETDAL BAKHIET

ID Number   : MSK17002

Date   : JANUARY 2021

BIOMINERALIZATION OF HYDROXYETHYL CELLULOSE/SODIUM ALGINATE IMPREGNATED WITH CELLULOSE NANOCRYSTALS BY USING SURFACE MODIFICATION TECHNIQUE

ETDAL BAKHIET

Thesis submitted in fulfillment of the requirements
for the award of the degree of
Master of Science

Faculty of Industrial Sciences and Technology
UNIVERSITI MALAYSIA PAHANG

JANUARY 2021

ACKNOWLEDGEMENTS
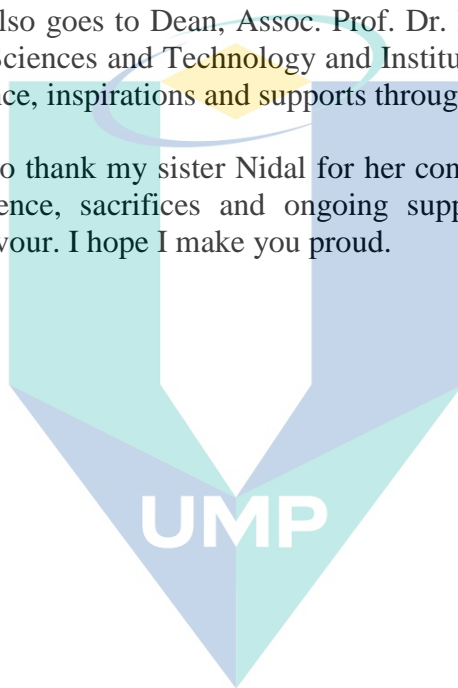
ABSTRAK

Kejuruteraan tisu tulang menghasilkan replikasi kerangka daripada pelbagai material biopolimerik untuk mendapatkan topographi tertentu dan pembenihan sel-sel tertentu sebelum dilaksanakan ke dalam badan yang cedera. Tujuan utama penyelidikan ini adalah untuk sintesis bahan biopolimer daripada hidroksil etil selulosa (HEC) (5% berat) yang dicampur dengan natrium alginat (SA) (10% berat) pada nisbah 1: 1, digabungkan dengan nanokristal selulosa (CNC) (11 w/v %) dan direka menggunakan teknik pengeringan beku. Tingkah laku peran cah seperti struktur kimia dan sifat terma diciikan dengan menggunakan FESEM, EDX, ATR-FTIR and UTM.. Pencirian adalah penting untuk memahami sifat fizikal, kimia dan mekanik kerangka. Biokompatibiliti in vitro kerangka telah disiasat dengan pengkulturan sel osteoblas janin manusia (hFOB) pada kerangka ini. Hasil imej SEM dipaparkan struktur berliang yang saling berkait dengan diameter antara 40 hingga 400 μm dengan peratusan keliangan dalam julat 75 ± 5% hingga 90.5 ± 5%. Pengembangan ratio yang ketara pada HEC/SA tidak dirawat denagn kerangka SBF disebabkan kekuatan ikatan hydrogen dan interaksi antara Van der Waals dengan rantai polimer. Kerangaka mula hancur selepas hari ketujuh yang mana berat menurun sehingga ~60%. Kemungkinan, ditu njukkan oleh ATR-FTIR disebabkan oleh interaksi diantara HEC, SA, dan CNC dalam campuran. Hasil TGA menunjukkan empat bahagian yang berlainan kehilangan jisim, mewakili suhu peralihan amorfus dan pelupusan air, pecahan ikatan rantaian sisi, pirolisis SA dan kelakuan dehidrosilasi kalsium fosfat. Interaksi sel menunjukkan sel hFOB menunjukkan perbezaan merebak sangat baik ke atas percambahan sel dan lebih menonjol terhadap HEC/SA/CNC yang dirawat dengan kerangka SBF. Oleh kerana biokompatibil dan terbiodegradasi ini menghasilkan keputusan yang baik, kerangka ini boleh digunakan untuk reka bentuk kejuruteraan tisu tulang yang akan dihasilkan oleh generasi akan datang..

ABSTRACT

Bone tissue engineering utilizes scaffolds fabricated from various biopolymeric materials to obtain a specific topography prior to seeding with specified cells and implantation into an injured body. The aim of this research is to synthesize biopolymeric materials from hydroxylethylcellulose (HEC) (5 wt%) blended with sodium alginate (SA)(10 wt%) at 1:1 ratio and incorporated with cellulose nanocrystals (CNC) (11 w/v%). The scaffolds was fabricated using the freeze-drying technique. For the mineralization process, these HEC/SA and HEC/SA/CNC scaffolds were treated with simulated body fluid (SBF) by immersion technique through the depositing of calcium phosphate on the scaffold's surfaces. The behavior of scaffolds such as chemical structures and thermal properties were characterized by using FESEM, EDX, ATR-FTIR, and UTM. In-vitro biocompatibility of the scaffolds was investigated by culturing human fetal osteoblast (hFOB) cells on these scaffolds. The SEM images displayed interconnected porous structures with diameters ranging from 40 to 400 μm and porosity percentages ranging from $75 \pm 5\%$ to $90.5 \pm 5\%$. The high swelling ratio of HEC/SA untreated with SBF scaffold was ascribed to the strong hydrogen bonding and Van der Waals interactions between polymer chains. After 7 days of incubation, the scaffolds began to disintegrate, which leads to the increase in weight loss (simultaneously up to ~60%). ATR-FTIR results exhibit possible interactions between hydroxyl groups of HEC, SA and CNC in the blends suggests there is chemical interaction between scaffolds. The TGA results showed four different regions of mass losses, represents the degradation temperature and water disposal, side-chain bond breaking, pyrolysis of SA and dehydroxylation behavior of calcium phosphate, respectively. The cell-scaffolds interaction demonstrated that hFOB cells differentiated and spread well on the scaffolds with better cell proliferation and attachment on HEC/SA/CNC treated with SBF porous scaffolds. Since these biocompatible and biodegradable scaffolds showed promising results, these scaffolds could be adopted for the design of next-generation tissue-engineered bone grafts.

TABLE OF CONTENT

LIST OF TABLES

LIST OF FIGURES

LIST OF SYMBOLS

Ca^+	Calcium ion
°C	Degree Celsius
W_d	Dry weight
ΔH_f	Enthalpy of fusion
ΔH_f^o	Enthalpy of fusion of 100% crystallization
T_g	Glass transition temperature
ΔH_m	Heat of fusion
W_o	Initial weight
L	Length
T_m	Melting temperature
μm	Micrometer
ml	Millilitre
T	Temperature
V_1	Volume of the scaffold before immersion
V_2	Volume of the scaffold after immersion
V_3	Volume of the scaffold after drying
E	Young's modulus

LIST OF ABBREVIATIONS

ATR-FTIR	Attenuated total reflectance Fourier transform infrared spectroscopy
CNC	Cellulose nanocrystals
DMEM	Dulbecco's modified eagle medium
ECM	Extracellular matrix
GA	Glutaraldehyde
GAG	Glycosaminoglycan
HA	Hydroxyapatite
HEC	Hydroxyethyl cellulose
hFOB	Human fetal osteoblasts
PBS	Phosphate buffered saline
PCL	Polycaprolactone
PE	Poly(ethylene)
PEO	Poly(ethylene) oxide
PGA	Poly (lactic) acid
PLA	Poly (lactic-co-glycolic acid)
PVA	Poly (vinyl) alcohol
SA	Sodium alginate
SEM	Scanning electron microscopy
TCP	Tri-calcium phosphate
TGA	Thermogravimetric analysis
UTM	Universal testing machine

CHAPTER 1

INTRODUCTION

1.1 Background

The interdisciplinary field of tissue engineering combines multiple knowledge concepts that allow the artificial cellular scaffold to preserve or rejuvenate the destroyed tissues; it involves manufacturing of materials with appropriate biochemical characteristics (Agarwal et al., 2009; Rodrigues et al., 2011) In tissue engineering, scaffolds are defined as an assist that imitates the extracellular matrix (ECM) while simultaneously serving as a provisional skeleton for cell attachment, proliferation and differentiation; it aids the reconstruction of new organs and tissues. A key factor for a model scaffold for bone tissue regeneration should possess proper surface chemistry, as well as microstructure with adequate mechanical properties, biocompatibility and bioactivity (Rodrigues et al., 2011). As a result, a prerequisite for development of such scaffold involves the proper selection of materials that meet the above criteria; such material must also be nontoxic to cells in both its original and degraded forms (Martins et al., 2007).

The bone hierarchy is divided into macro and nano-sized tissues which are highly vascularized connective tissues with regenerative capacity throughout the lifetime of an individual. Bone provides body movement and serves as a supportive casing for the delicate internal organs. However, problems like bone injuries, loss and deficiencies tend to increase on a daily basis, thereby triggering the need for growth of a wide diversity of man-made materials for bone repair and regeneration. The main purpose in utilising the synthetic bone scaffolds for orthopaedic treatment are due to eliminate donor site morbidity, overcome the issue of inadequate bone tissue quality, and to reduce the risks of disease transmission. Furthermore, the use of synthetic scaffolds would lead to fewer surgical procedures, and can also help to eliminate the risk of infection or immunogenicity (Porter et al., 2009).

Over the last few decades, bone tissue engineering has incorporated several inbred and man-made polymers, as well as their blends. Notable among these are collagen, chitosan and chitin which are among the most broadly used natural polymers. Due to the structural and functional resemblance of collagen to natural bone extra cellular matrix, it initially attracted much research interest as a potential bone scaffold (Sheehy et al., 2014; Cen et al., 2008). However, the high cost of collagen led to its gradual replacement with gelatin-based materials which hold brilliant biodegradability and non-antigenicity. However, gelatin exhibits lower mechanical strength. (Cen et al., 2008).

On a more general note, it has been observed that when scaffolds are processed into nano-scale, natural polymers often lack the sufficient mechanical strength required for applications in bone tissue engineering (Yang et al., 2008; Kanungo et al., 2008; Cen et al., 2008). Therefore, polyesters such as polylactic acid (PLLA), polyglycolic acid (PLGA) and polycaprolactone (PCL) which are a common group of manmade polymers are currently being used to construct biodegradable nano-fibrous materials for bone tissue engineering (Heydarkhan-Hagvall et al., 2008; Kong et al., 2006). One problem of these materials is that their degradation rates are often high and their degradation products are usually acidic. Additionally, these materials sometime involve toxic chemicals as solvent during their preparation (Goonoo et al., 2013).

Among the common materials with potential use in bone engineering, hydroxyethyl cellulose is of particular interest. Hydroxyethyl cellulose (HEC), has many advantages as it is derived from cellulose. It has β (1→4) glycosidic linkage and chemical structure that is comparable to glycosaminoglycans (GAGs) and polysaccharides. Furthermore, it is biocompatible, biodegradable, water soluble, non-toxic, non-ionic and cost effective. On the other hand, sodium alginate (SA), a polysaccharide product, is widely used in drug delivery and ECM scaffolds. It is biocompatible, biodegradable and abundant at an affordable price; these made it attractive for tissue engineering.

In this regards, one promising approach is tissue engineering method in which employing a bioresorbable and biodegradable material scaffold to engineer the repair of

bone tissues. This has been observed to be highly effective because scaffolds act as extra cellular matrix (ECM) to organise cell and to present stimuli which facilitates the formation of growth of the desired tissue. Hence, the cellular growth and tissue development are often contingent on the characteristics of the scaffolding system, especially its structure and chemical composition (Liao et al 2008).

In this research, the HEC/SA scaffolds are incorporated with CNCs and fabricated via freeze-drying technique. The physical, chemical, mechanical, and thermal properties of the scaffolds were characterized using SEM, ATR-FTIR, TGA, and mechanical testing. In-vitro degradation and cell culture studies were also carried out to investigate the biocompatibility of cell-scaffolds and their potential as a substrate for bone tissue engineering; this was validated using MTS assay and morphological studies.

1.2   Problem Statement

The emergence of tissue engineering has rejuvenated the conventional autograft, allograft and xenograft techniques in order to remain, restore or/and improve tissue functions. Numerous studies have been done by utilizing biopolymer materials fabricated via various techniques, such as electrospinning, freeze-drying, solvent casting, phase template and many others. Through these techniques, scaffolds characteristics can be modified to produce an ideal scaffold that possesses good biodegradability, biocompatibility and mechanical properties for tissue regeneration (Pangon, 2016). Nowadays, bone graft tissue engineering has succeeded in bringing an alternative solution to patients with bone diseases, including osteoporosis and bone fracture due to aging, trauma and accidents. Many available bone grafts are currently available in the market; however, there are several limitations of such grafts, such as high cost, environmental toxicity, inappropriate biodegradable rate, and weak mechanical properties (Martin et al., 2018).

Furthermore, a good scaffold must not elicit immune reaction to prevent inflammatory response that could reduce healing. Therefore, the development of new bone tissue scaffolds with adequate mechanical properties and capacity for vascularization is important. Many researches have confirmed that bio composite

materials could offer significant improvements that can help to overcome some of the inherent problems of scaffold materials (Liu et al., 2017; Wang et al., 2017). Previous studies showed that the use of hydroxyethyl cellulose improved the percentages of porosity of scaffolds but lowered the mechanical strength. However, the addition of HEC with other polymers proved to boost the bioactivity, mechanical properties and helped in protein adsorption, thereby increased cell availability and proliferation (Tohamy et al., 2018). Various parameters are considered during scaffolds fabrication based on the targeted tissue formation and functionality. (Zhou et al., 2016) modified the collagen network surface by coating with calcium phosphate (CaP) for biomimetic mineralization; this increased the mechanical strength of the resulting material.

The incorporation of this biomineralize element was proved to enhance the stability of the scaffold; however, the optimized concentration remained indistinct. In the other hand, studies from (Zhang et al., 2015) reported that the integration of cellulose nanocrystals into silk fibroin/carboxymethyl chitosan could increase strength and enhance protein absorption, and alkaline phosphate activity. However, the issues of less interconnected pore structure and porosity have limited the potential scaffolds fabrication. Due to these gaps, this study exploited the advantages of cellulose nanocrystal, as well as the formation of calcium phosphate by surface modification to improve the biocompatibility and strength of scaffolds for tissue engineering application.

1.3   Objectives

The main objectives of this research are as follows:

i.   To synthesize porous scaffolds of HEC/SA, HEC/SA/CNC, HEC/SA (SBF) and HEC/SA/CNC (SBF) scaffolds using a freeze-drying technique.

ii.   To study the physical, chemical, mechanical and thermal properties of synthesized scaffolds.

iii.   To investigate the in-vitro cell culture performance of the synthesized scaffolds for possible use as bone grafts.

1.4 Research scope

To achieve objective (i), the research scopes include:

i. To prepare polymer blends of HEC and SA incorporated with CNC.

ii. To modify the surface of HEC/SA/CNC scaffolds by immersion technique in SBF solution.

iii. To optimize the parameters (temperature, pressure and time) used for the fabrication of porous materials during the process of freeze drying.

To achieve objective (ii), the research scopes include:

i. To observe the surface morphology of all the scaffolds via SEM, and to measure the pore size by using ImageJ software.

ii. To analyse the swelling behaviour, porosity and biodegradability of the scaffolds.

iii. To identify the functional groups of the scaffolds using ATR-FTIR spectra.

iv. To study the thermal stability and decomposition behaviour of the scaffolds using TGA.

v. To study the mechanical strength of the scaffolds by analysing the stress-strain curves using UTM.

vi.

To achieve objective (iii), the research scopes include:

i. To investigate the cellular biocompatibility by carrying out in-vitro cell culture studies using human fetal osteoblast (hFOB) cell.

ii. To determine the adherence, differentiation and proliferation of hFOB cells on the scaffolds using MTT assays based on the measurement of the absorbance values, and to observe the surface morphology changes by SEM.

iii. To identify the optimum concentration of CNCs in HEC/PVA scaffolds that display better response towards hFOB cells.

1.5   Significance of Study

The proposed research work is related to fabrication of porous scaffolds with good morphological structure, high porosity, excellent cell-scaffold biocompatibility, osteoconductivity, biodegradability, and good mechanical strength.

i.   Novel porous scaffolds were produced from HEC, SA and CNC treated with SBF for use as potential scaffolds in bone tissue engineering.

ii.   Scaffolds were produced via a green technology that involved water as the only solvent.

iii.   Overall, this research fully supports the conversion of waste to wealth.
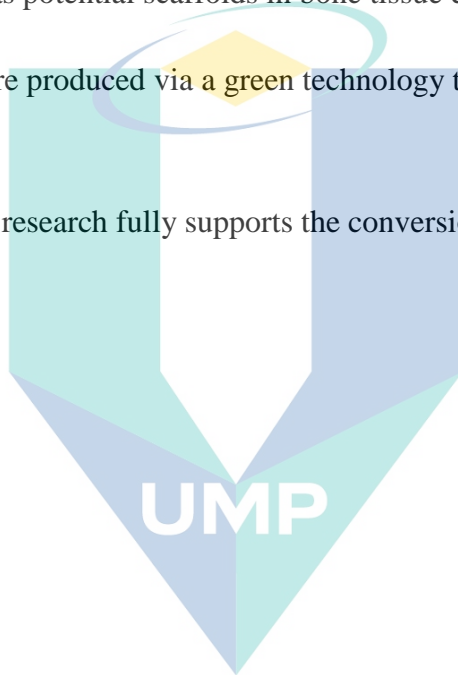
CHAPTER 2

LITERATURE REVIEW

2.1   Human bone physiology

Bone comprises mainly three types of cells - osteoblasts, osteoclasts and osteocytes. With respect to individual function, osteoblasts generate new bones while osteoclasts are responsible in maintenance, repair and modelling of bones (Sanchez et al., 2018). Meanwhile, the osteocytes brings support to mechanical strain and send the signals of bone formation or bone resorption to the bone surface. (Martin & Sims, 2015). In general, biomineralized bones play many roles, including provision of support to posture, maintenance of body structure, protection of internal organs, and facilitation of body movement.

2.1.1   General function of bone

Skeletal bones act as a support structure against gravity, as a pedal system for the muscles, and as a protection for the internal organs (Tomlinson et al., 2016). Bone is a complex biphasic material which consists of a firm phase that involves bone cells embedded in an extracellular matrix that includes hydroxyapatite crystals for the strengthening of bones (Miranda-Nieves & Chaikof, 2016). Bone also serves as a reservoir of minerals. Patient's lifestyle and medications are believed to impact bone health (Hopkins et al., 2016).

Bone extra cellular matrix (ECM) is made up of nanoscale organic constituents that include collagen and non-collagenous proteins and hard inorganic nano-hydroxyapatite (nHA) (Geng et al., 2009). The inorganic mineral composition of bone is comprises of calcium, phosphates, carbonates and hydroxyl components and contribute towards good mechanical strength and osteoconductivity (Ngiam et al., 2009). On the other hand, the organic component of extracellular matrix contains a variety of protein

fibrils and fibres intertwined within a hydrated network of glycosaminoglycan chains. This network structure functions as a scaffold which can support tensile and compressive stresses through the help of the fibrils and hydrated networks. It is noteworthy that the fibrillary and porous structure of ECM have a great influence on cell functionality, particularly on cell adhesion and migration.

Beyond provision of an applicable microenvironment for cells, ECM is responsible for transferring signals to cell membrane receptors that reach nucleus via intracellular signalling cascades (Tuzlakoglu et al., 2005). In addition, they support cell and tissue differentiation, cell proliferation, cell adhesion, cell migration, tissue regeneration and repair (Shin et al., 2007). Ideal scaffolds should be biocompatible, biodegradable, and promote cellular interactions and tissue development, and possess proper mechanical and physical properties. Furthermore, the scaffolds must have a porous design, produce non-toxic degradation products, and should be capable of sterilization without loss of bioactivity and should deliver bioactive molecules in a controlled fashion to accelerate healing (Venugopal et al., 2008).

2.1.2 Structural and mechanical properties of bone

There are two types of bone at a microscopic scale - compact and cancellous bone, as in Figure 2.1 (a) which showed the outside of the bone, while Figure 2.1(b) showed the physiological structure of the bone. The bone is organised in concentric layers around canals, forming structural units called osteons (Han et al., 2017). Compact bone or cortical bone is a dense material that makes up mostly the shaft (Cooper & Maas, 2018). It is a solid part which forms a shell around the spongy bone, as shown in Figure 2.2. Meanwhile, cancellous bone, also called trabecular bone, is a porous material that makes up the epiphysis of a long bone (Wang & Yeung, 2017). The cancellous bone is made up of very light parts with an open pore section filled with marrow, and blood vessels that carry cell and nutrients in and out of the bone.
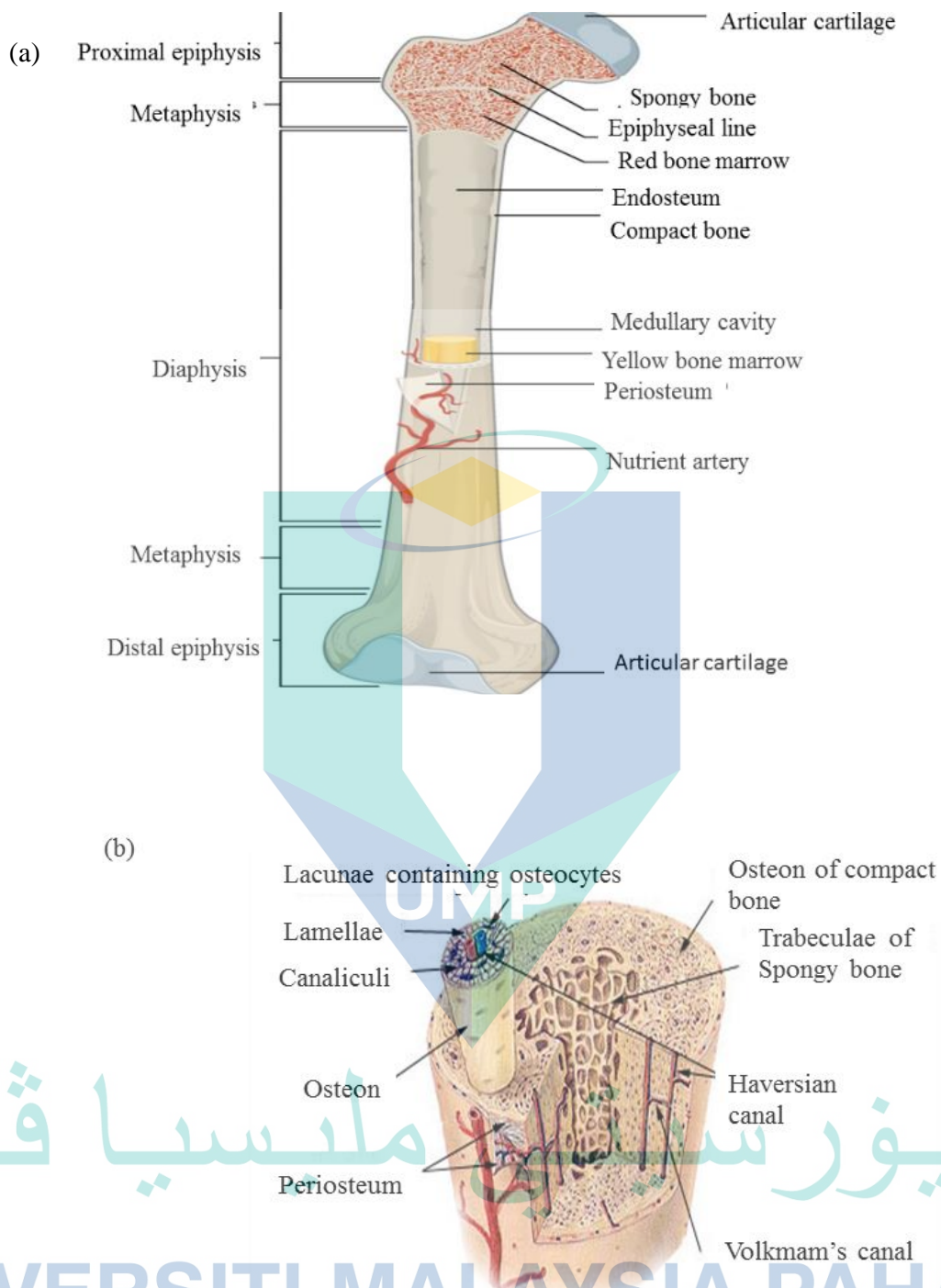
Figure 2.1   Cross-section image of (a) bone structure and (b) physiology of bone
Source: White & Folkens (2005).
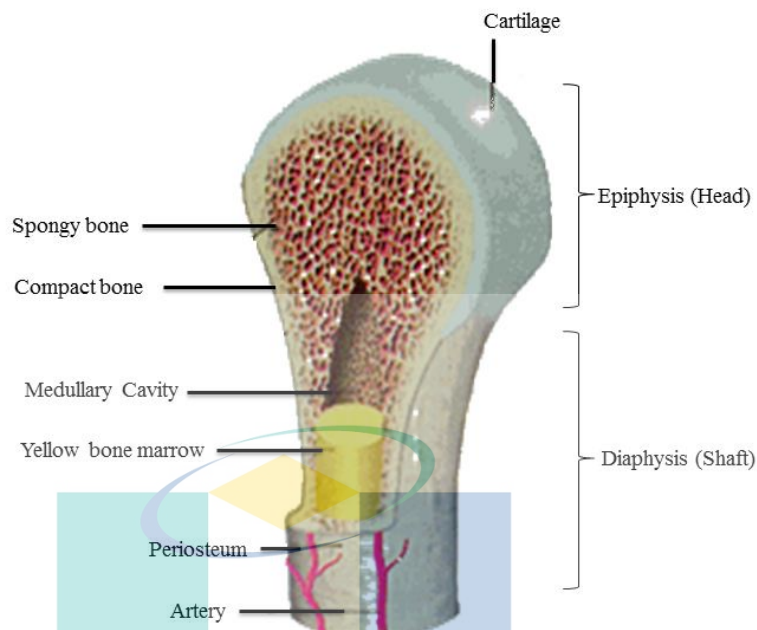
Figure 2.2   Cross-section image of compact and spongy bone physical structure
Source: White & Folkens (2005).

In this research, the scaffolds will be fabricated by using freeze-drying technique to produce a sponge-like pore structure similar to spongy bone. Therefore, understanding the composition of human bone and mechanical properties of human spongy bone is very important. Table 2.1 showed the mechanical properties of human spongy bone in terms of its tensile stress, compressive stress, and elastic modulus.

Table 2.1   Mechanical properties of human spongy bone

Mechanical Properties	Strength	Reference
Tensile strength	10-20 MPa	(Wu et al., 2014)
Compressive strength	2-12 MPa	(Wu et al., 2014)
Elastic modulus	1-5 GPa	(Wu et al., 2014)

2.2   Bone tissue Engineering

Bone tissue engineering, applies the principles of biology and engineering to the development of variations substitutes that regenerate, restore, maintain, or improve the function of tissues and bone (Chinnappan et al., 2018). Bone tissue engineering aims at designing, safe and sustainable functional bone tissues by making more informed choices based on our improved understanding of human bone structure, mechanics, and tissue formation. It has revolutionized the biomedical field by resolving the recurrent limitations of obsolete conventional methods: autograft, allograft, and xenograft, in healing bone defects by possess a healing strategy to cure the injured organ (Gómez et al., 2016; Vig et al., 2017). The autograft possesses several drawbacks such as limited grafts supply, prolonged healing, increased pain and morbidity. On the other hand, allografts are an adequate substitute for autograft but are immunogenic and suffer from graft rejection and disease transmission risk. Alternatively, xenograft has been used by surgeons by surgical grafting from one species to another species, wherein the rejection and autoimmune disease are possible outcomes of this type of graft.

2.3   Characteristics of biomaterials scaffold

The structural and behaviour characteristics of tissue scaffold including physical, mechanical, chemical and biological are critical to ensure normal cell activities and performance during cell cultivation (Rezaei & Mohammadi, 2013). The ideal scaffold should meet the physiological demands of native extracellular matrix (ECM) in order to promote excellent host-cell mediated healing (Barnes, 2007). The characteristics of biomaterials scaffold is vary depending on the type of materials and the tissue types where the scaffold is to be applied (Yang et al., 2001).

First of all, all scaffolds should be biocompatible which is neither the biomaterials nor its degradation by-products should provoke any rejection, inflammation or immune responses (Chen e al., 2002). The scaffold should provide three-dimensional structure with interconnected porous architecture to assist cellular ingrowth and facilitate nutrients and oxygen delivery (Deluzio et al., 2013 ; Leukers et al., 2005). The three-dimensional scaffolds should be able to initiate cell attachment and subsequent tissue formation to ensure the cell adheres and proliferates into the structure.

11

The biomaterial scaffold should also be biodegradable upon implantation at a rate matching of that new tissue regeneration (Chan & Leong, 2008).

In addition, the scaffold should provide adequate mechanical properties consistent with site into which it is to be implanted and bear strong enough biological forces to allow surgical handling during implantation (Brien, 2011). The biomaterial scaffold should exhibit high surface area to support better cell adhesion, promote cell growth and allow the retention of differentiated cell function (Chen e al., 2002). The scaffold should also have surface roughness similar to native tissues for enhanced tissue-scaffold interaction (Zhao et al., 2013). Furthermore, the scaffold should be vascular supportive to provide channels for adequate blood supply for rapid and healthy tissue regeneration (Zhang & Michniak-Kohn, 2012). Finally, the biomaterial should be stable during storage and must be sterilizable in order to avoid any contaminations, without compromising any structural or other related properties (Ramakrishna et al., 2016). Despite of above discussed properties, it should be noted that the success of biomaterial scaffold is also depends on many other factors such as implant design, surgical techniques, health conditions and activities of the patient.

2.4   Classification of biomaterials

Osteoinductive biomaterials, including natural and synthetic polymers, have the ability to form bones by inculcating its surrounding in-vivo environment. While the biological mechanisms of this wonder are yet to be clarified, it is widely accepted that these materials present significant potential (Li et al., 2017). The characteristic and chemical properties of natural polymers (chitosan, alginate, fibrins) showed increased osteoconduction, osteoblast attachment, and presence of growth factors. Natural polymers include collagen, gelatin, silk and chitosan as in Figure 2.3 (a), (b), (c) and (d), respectively (Ahmed & Ikram, 2016). These types of polymers are derived from plant or animal-based sources and are generally referred to as renewable resources polymers; they are biocompatible and bio-degradable (Stratton, Shelke, Hoshino, Rudraiah, & Kumbar, 2016). For example, chitosan which is found in the cell walls of fungi can also be derived from chitin by deacetylation process. While collagen is a protein with fibrils that provide mechanical strength to the cell wall (Yamamoto et al., 2017). It is a mixture of proteins and peptides with chemical structure similar to

collagen (Shaabani et al., 2016). Sodium alginate can be mixed with other polymers to alter its physical, chemical, and mechanical properties for specific applications (Wang et al., 2019).
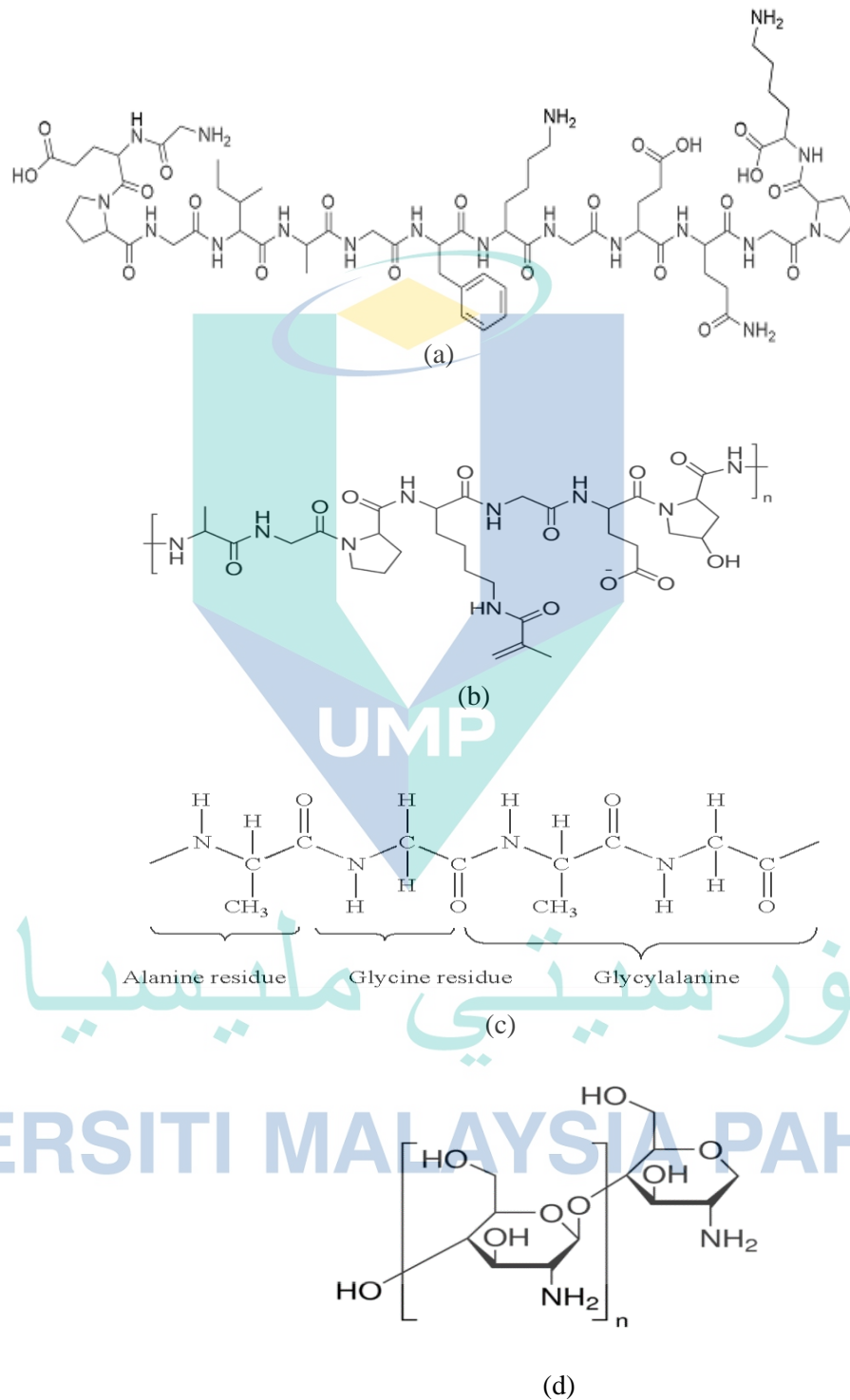
Figure 2.3   Chemical structure for (a) collagen type-II, (b) gelatin, (c) silk fibroin, (d) chitosan

Apart from natural polymers, the man-made or synthetic polymers as shown in Figure 2.4 (a), (b), (c) and (d). have also been used to manufacture biomaterials for biomedical applications, specifically in tissue repair and drug delivery. Poly (vinyl alcohol) (PVA) is among the alternative synthetic polymers, shown excellent function as polymer matrix and widely design to be incorporated with nano-substrates to enhance the cells-scaffold biofunctionality (Hakkou et al., 2019). Other polymers such as polycaprolactone (PCL) is a biodegradable polyester with suitable mechanical properties, while poly(lactic-co-glycolic acid) (PLGA) and poly(ethylene) oxide (PEO) is a polyester that are commonly suggested for medical uses due to their low toxicity and water solubility (Pourasghar et al., 2019). In addition, poly(lactic acid) (PLA) that derived from renewable plant sources, such as starch and sugar possess excellent biodegradability and biocompatibility owing to its design flexibility and surface modifiability (Stratton et al., 2016).

Several researchers have used different types of biomaterials, including ceramic but this type of biomaterial has some limitations, such as insufficient elasticity and cracking which encouraged researchers to use natural polymers which showed weak mechanical properties. The synthesised material also displayed no binding sites. Recently, the hybrid materials which consist of a multiple synthetic and natural polymers, including ceramics, have been developed and recognised as biomaterials for bone tissue engineering (Catauro et al., 2015). Biomaterials for bone scaffolding applications such as, poly (lactide-co-glycolide) (PLGA) co-polymer systems, derived from poly lactide shows a glass transition temperature with a longer degradation time, while polyglycolide, shows a transition temperature with shorter degradation time. In polymer blends, the process involves in the mixing of two polymers with intermolecular or Van der Walls interactions contribute in enhanced properties of the designed biomaterial. PLGA blends with polyphosphazenes illustrates a good physicochemical and osteo properties if compared to the non-blend polymer (Ribeiro et al., 2015).
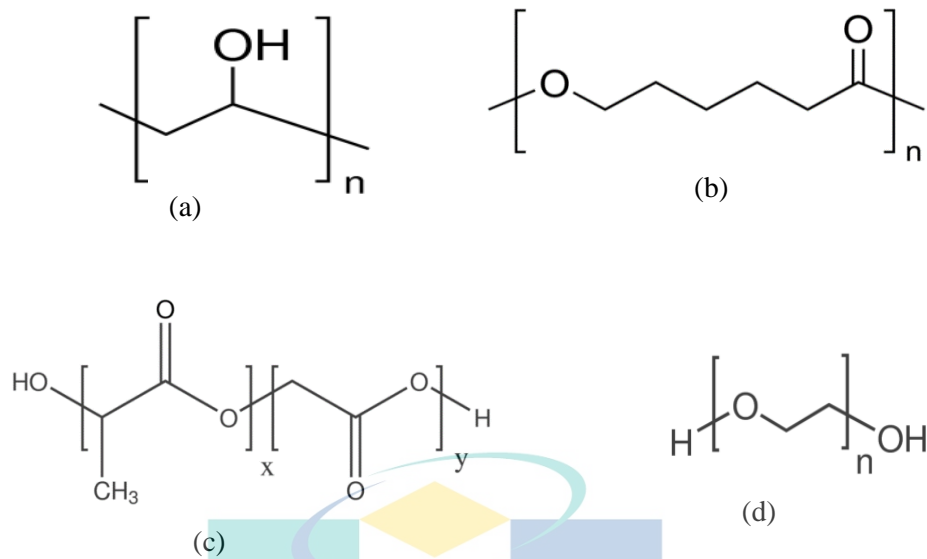
Figure 2.4   Chemical structures of (a) PVA, (b) PCL, (c) PLGA, (d) PEO

In addition, biomaterials include polymer-ceramic composites that represent smart contestants for bone tissue engineering applications, for instance, composite materials comprising of a mix of inorganic hydroxyapatite crystals and organic collagen fibres exhibit excellent biological properties for bone growth (Affatato et al., 2015). The study used black phosphorus incorporated PCL and collagen nanofiber matrix and the results indicated that the biocompatibility and bio functionality of the produced scaffolds improved cell attachment and proliferation (Lee et al., 2019).The appliance of composite materials fulfil the biological requirements, such as biocompatibility, biodegradability and bio restorability. Moreover, the structural features of scaffold with some modification enable the fabrication of porous scaffolds for bone regeneration and tissue replacement (Yin et al., 2018; Cox et al., 2015).

Other type of biomaterials is the hydrogels scaffolds which have a number of features resulting in their unparalleled biocompatibility and unique physical characteristics. Hydrogels scaffolds have long been used as materials for tissue engineering. Hydrogels not only serve as matrices for tissue engineering and regenerative medicine but are also able to emulate ECM topography and deliver required bioactivity. Immunomodulatory approaches aim to produce biomaterials that can improve or control the immune system in a favourite manner for enhanced bone repair and regeneration. Usually, the host's immune reaction to an implant begins with

15

the initial acute response to the surgical injury and essential recognition of the foreign material, which later results in the modification of immunity responses (Vrana, 2016)

2.5   Fabrication of biomaterials

There are various method of scaffolds fabrication, such as particulate leaching, electrospinning, rapid prototyping and freeze drying techniques (Ali & Lamprecht, 2017). Techniques such as particulate leaching enable to control the inner architecture of scaffolds. It is functionalized by embedding the salts in the polymer matrix and consequently filtered out to leave interconnected internal channels. Thus, by regulating the size of the salt particles, the pore diameters of the scaffolds can be controlled; however, the agglomeration of salt particles can alter the eventual pore size and pore distribution during leaching (Rem et al., 2020).

In the interim, electrospinning has become tremendously desired technique possibly due to the recognition in nanotechnology such as ultrafine fibers or fibrous structures of various polymers with diameters up to nanoscale which can be straightforwardly fabricated in a short period (Chinnappan et al., 2018). The rapid prototyping technique has emerged as an innovative process of manufacturing with an intrinsic capability to create objects in virtually any shape with increased speed than before. This technique, combining computer-aided design (CAD) with computer-aided manufacturing (CAM), has the distinct advantage of being able to build objects with predefined microstructure and macrostructure (Liu et al., 2017). This distinct advantage gives beneficial potential for making scaffolds or orthopaedic implants with controlled hierarchical structures (Limongi et al., 2017).

The freeze-drying method or lyophilization has been used to fabricate porous scaffolds and has been widely investigated in tissue engineering fields. Freeze-drying enable the fabrication of highly interconnected porous 3D scaffolds and could be produced in bulk, yet suitable for histological sections (Ali & Lamprecht, 2017). Freeze-drying, also known as lyophilization has been utilized since 1250 BC as a method of preserving food. In early 1980s, Altman once reported the used of freeze-drying method in the preparation of histological sections (Meryman, 1976). Nowadays, freeze-drying is one of the techniques to fabricate porous scaffolds and has been widely investigated for the last two decades in tissue engineering field (Subia et al., 2010). It is

a common method for producing large and highly interconnected porous 3D scaffolds that can be performed with dissolved synthetic and natural polymers including silk, collagen, PGA, PLLA, PLGA, PLGA/PPF blends (Schoof et al., 2001; Vepari and Kaplan, 2007; Altman et al., 2003) . Freeze-drying involves three major steps: Firstly, the solution is frozen at a low temperature usually in range of −50°C to −80°C, then, the frozen sample will undergo the primary drying process in which the sample is located in a chamber through a partial vacuum with the pressure is lowered to a few milibars in which the ice in the material is removed by direct sublimation while the final stage which is secondary drying process, removed most of the unfrozen water in the material by desorption (Lu et al., 2013). The main advantage of this technique is it neither requires high temperature nor separate leaching step (Subia et al., 2010). The drawback of this technique is long processing time, low mechanical stability, sensitivity of the technique where the processing parameters have to be very well controlled and small pore sizes in the range of 100 µm (Hutmacher, 2000; Yang et al., 2001).

2.6   Materials study

2.6.1   Hydroxyethyl cellulose

Hydroxyethyl cellulose (HEC) is an important derivative of cellulose with a chemical structure which is similar to glycosaminoglycans (GAGs). HEC is a non-ionic water soluble derivative of cellulose ethers with low charge density, mainly used as stabilizers and thickeners in paint preparations, hair and eye-care solutions, as protective colloids in polymerization processes and in paints to make it thick (Zhao et al., 2018). The chemical structure of HEC is as shown in Figure 2.5. HEC has a hydrophilic behaviour with polysaccharide biopolymers with β $(1 \rightarrow 4)$ glycoside linkage. HEC is modified from cellulose base by replacing ethyl group with hydroxyl groups, which are present in each glucopyranoside. This is used as a soluble intermediate for processing cellulose into sponge, fibre and film forms. The degree of substitution and their relative distribution in different carbon positions 1, 2 and 6 have strong effect on the properties and behaviour of these polymers. Prior study used a combination of hydroxyethyl cellulose, soy protein isolate, crosslinking and freeze-

drying to produce scaffolds; the results specified that the composite sponges demonstrated zero cytotoxicity and might support cell proliferation and cell attachment.
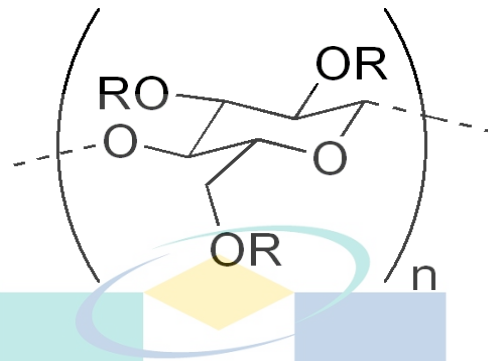
Figure 2.5   Chemical structure of hydroxyethyl cellulose

2.6.2   Sodium alginate

Sodium alginate (SA) is the sodium salt form of alginic acid and gum mainly extracted from the cell walls of brown algae. SA has a white to yellow powder appearance. It is a polyelectrolyte compound with biocompatible properties and this compound is widely applied in the scope of biomedical. SA has been widely used as a copolymer to produce blended polymer scaffolds. However, SA has a poor process ability and the synthesis of nanofibers is hard to conduct, due to its repulsive forces present and polyelectrolyte behaviour (Li et al., 2012). In order to improve its process ability, SA can be mixed with other polymers in order to alter its physical, chemical, and mechanical properties to achieve the desired application. The chemical structure of SA is as shown in Figure 2.6.
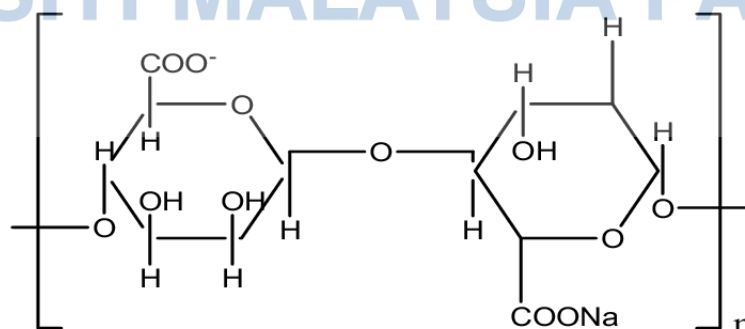
Figure 2.6   Chemical structure of sodium alginate

2.6.3 Cellulose nanocrystals

Cellulose nanocrystal exhibits a nanostructure in the kind of rod or needle-like structure which have a diameter range of 5-30 nm and length range of 1-100 nm (Figure 2.7). In general, several sources are used to produce cellulose nanocrystals, including oil palm, cotton, fibre, corncob, coconut husk fibre and rice peel (Chemin et.al, 2019). CNC provide better physical and chemical properties compared to its precursor such as it has a higher surface area ($\sim$250 m^2/g), high tensile strength (7500 MPa), high stiffness (Young's Modulus up to 140 GPa), abundance of reactive hydroxyl group on the surface and has a good biocompatibility (George & Sabapathi, 2015). During last two decades, the use of reinforcing agent including CNC have been an interesting topic and the effort done have been growing exponentially in annual basis. The need of the CNC is due to the plasticization in humid environment that limits the application of PVA-based component (Peresin et al., 2010). Other than that, the presence of -OH group in CNC causing it to be applicable for the production of composite with polar and hydrophilic polymer (Grishkewich et al., 2017) .; Grishkewich et al., 2017;;

Cellulose nanocrystals can be produced via an acid hydrolysis process, by releasing hydronium ions for hydrolytic division of glycosidic bonds in cellulose molecular chains along the cellulose fibrils. This process breaking down the hierarchical structure of the nanofibril packed into crystalline nanocrystals (Tang et al., 2017) Applications of CNC can be found in the bio-imaging or biosensor such as quantum dots (QDs which oxidized CNCs were used to prepare well-dispersed quantum dots by using one-pot synthesis (Chen, Liu, Lai, Berry, & Tam, 2015). Next, CNC also has been finalised as the good candidates to be used in the energy storage application in which (Wu et al., 2014) have been modified the CNC surface and carboxylic groups by using TEMPO mediated oxidization process to assemble them into batteries and super capacitors. Other than that, as the CNC is the nontoxic material and have high surface area, it has been used in the waste water treatment function as adsorbent that adsorb cationic dye and methylene blue in the maximum capacity to produce clean water (He et al., 2013).
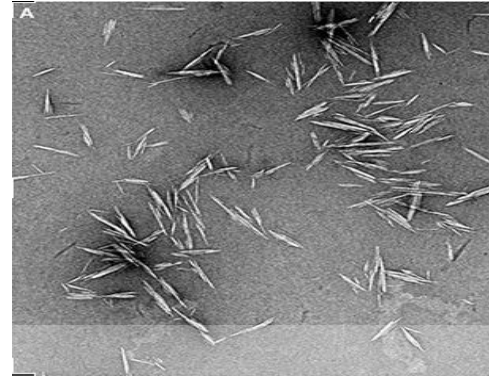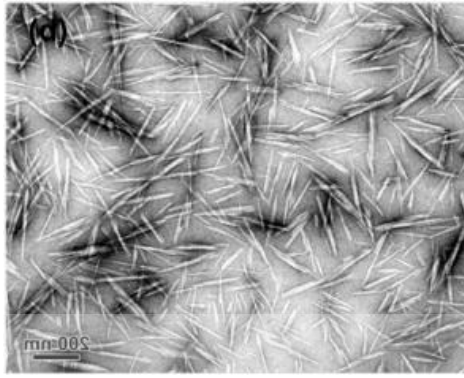
Figure 2.7   Needle-like structure of CNC

Source: Chemin et al. (2019)
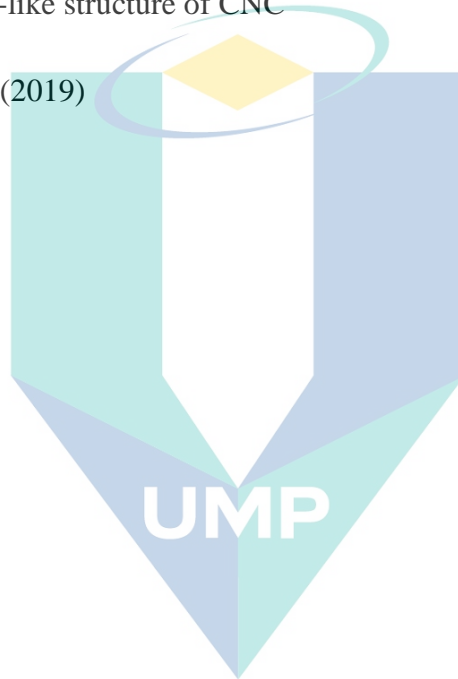
CHAPTER 3

METHODOLOGY

3.1   Introduction

This chapter presents the methods for the preparation of the samples for testing, and different characterization techniques. The fabrication method used in this research is lyophilisation or freeze-drying, followed by cross-linking and subsequently a bio-mineralisation process. The properties of chemicals used, and the methods used during the experiments are further clarified in this chapter. The flow chart of the experimental procedure is presented in Figure 3.1.
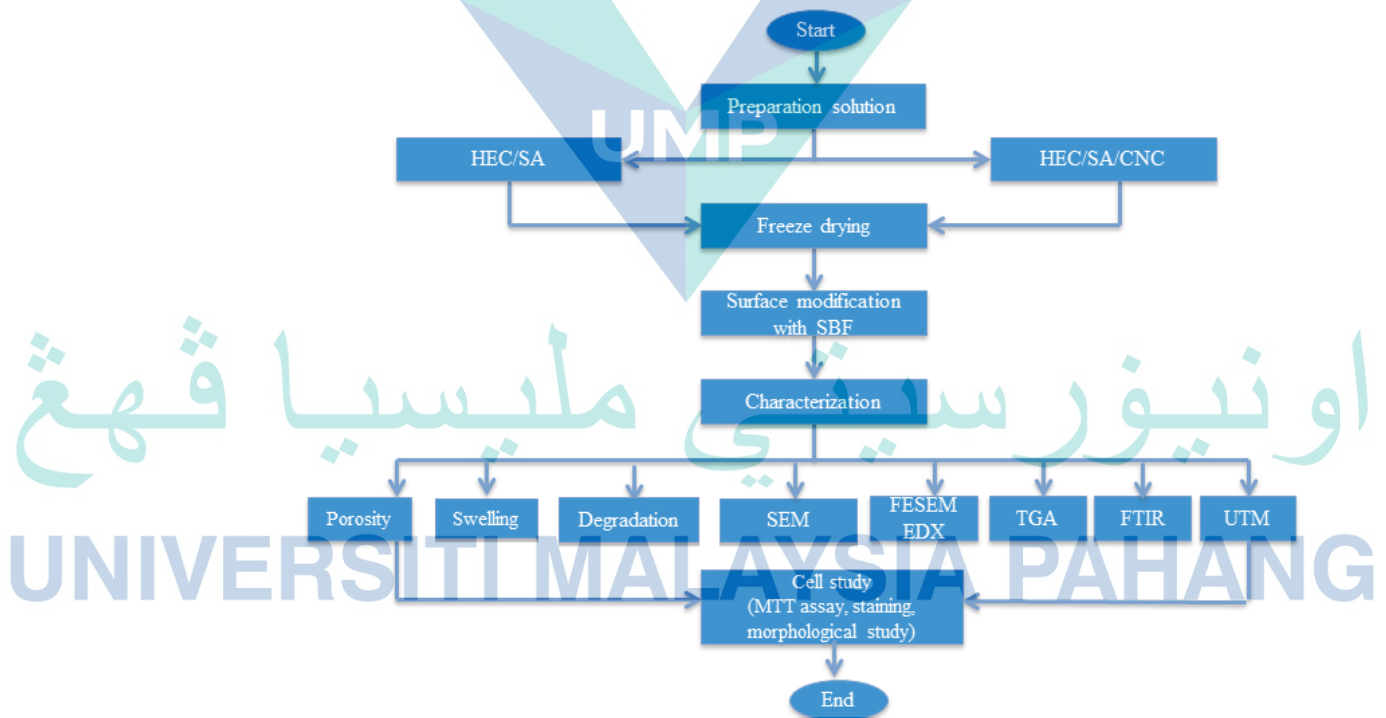
Figure 3.1   Flow chart of the research

3.2 Materials preparation

3.2.1 Raw materials

Sodium alginate, HEC (M_w = 250,000) and glutaraldehyde (GA) solution (25 %) were purchased from Merck-Schuchardt, Germany. Phosphate buffer saline (PBS) was purchased from Gibco Life Technologies, USA and Dulbecco's Modified Eagle Medium (DMEM) was purchased from Life Technologies, USA. Human fetal osteoblast (hFOB) 1.19 (ATCC® CRL¬11372™), SV4D large T-antigen transfected was supplied by American Type Culture Collection (ATCC), USA for cell culture studies. Cellulose nanocrystals used for this work were produced from empty fruit punch and obtained as a donation from the Faculty of Chemical Engineering in response to research team collaboration. All chemicals were analytical pure and applied without further treatment. All the solutions were prepared using Millipore water.

3.3 Preparation of HEC/SA/CNC and HEC/SA/CNC polymer solution

3.3.1 Synthesis of HEC/SA/CNC

Hydroxyethyl cellulose (HEC) solution of 5 wt% was prepared by dissolving 5 g of HEC powder in 100 mL of Millipore water at room temperature. The solution was then stirred for a period of 2 hours. Solution of sodium alginate (SA), 10 wt% was prepared by dissolving 10 g of SA powder in 100 mL of Millipore water at room temperature; the solution was then stirred for 2 hours. HEC/SA solution was formulated by mixing HEC with SA solution at weight ratios of HEC/SA, 1:1. HEC/SA/CNC was prepared by adding 11 wt % of CNC into HEC:SA solution. All solutions were stirred overnight to achieve homogeneous solutions.

3.4 Freeze-drying

Scaffolds were prepared by freeze drying method. The solution was poured into the container and kept in deep freezer at -80 ºC for 24 h. These frozen samples were lyophilised in Labconco freeze-dryer at -50 ºC for 72 h to obtain porous scaffolds. Subsequently, the scaffolds were kept in a chamber saturated with glutaraldehyde vapor for 72 h for crosslinking formation, undergo heat treatment at 140 ºC for 10 minutes and dried in a vacuum oven for a day.

3.5   Crosslinking process

The cross-linking process is a chemical and physical interaction which link one polymer to another via a covalent or an ionic bond. A ratio of 24 mL, 4 mL and 0.4 mL of acetone, glutaraldehyde, and phosphoric acid were used, respectively to carry out the cross-linking process. The scaffolds were crosslinked via vaporization technique by placing both scaffolds and crosslinker in the desiccator for 24 h. Thereafter, immersion testing was done to ensure its stability of scaffolds in water.

3.6   Surface modification with Simulated Body Fluid (SBF)

The simulated body fluid was prepared by the adding sodium chloride, sodium hydrogen carbonate, potassium chloride, di-potassium hydrogen phosphate trihydrate, magnesium chloride hexahydrate, calcium chloride, sodium sulphate with the concentrations of the ions were 2.5 times of normal SBF, which were 355.0 mM Na^+, 12.5 mM K^+, 7.5 mM Mg^{2+}, 6.25 mM Ca^{2+}, 369.5 mM Cl^-, 10.5 mM HCO_3^-, 2.5 mM HPO_4^{2-} and 1.25 mM SO_4^{2-}. The scaffolds were buffered to pH value of 7.2 at 37 ± 0.2 °C with Tris−HCl. The scaffolds were cut in a circular disc shape before immersed in SBF solution for up to 7 days. After day 7, the scaffolds were removed from the solution, rinsed with distilled water and dehydrated in an oven at 40 °C until constant weight.

3.7   Characterization technique

The morphological, chemical, thermal analysis and mechanical properties of the prepared scaffolds were investigated by using different techniques, such as scanning electron microscopy (SEM), attenuated reflectance transmission-Fourier transforms infrared spectroscopy (ATR-FTIR), thermogravimetric analysis (TGA) and universal testing machine (UTM). Other physical analysis conducted were porosity, swelling behaviour and degradation test. In addition, in-vitro biocompatibility of the materials was conducted through cell viability (staining) and cell proliferation analysis (MTT assays) by utilizing hFOB cells.

3.7.1 Scanning Electron Microscope

The scanning electron microscope (SEM) aids in observing and analysing the morphology of samples. SEM produces a magnified image by using an electron beam that's operated when the beam hits the sample and the electrons are converted to signals through the detector producing the image. The microstructures of porous scaffolds were investigated by using a scanning electron microscope (SEM) (ZEISS EVO 50; refer to Appendix 1) at an accelerating voltage of 10 kV. The dried scaffolds were sputter coated with a thin layer of platinum in 30 seconds consecutive cycles at 45 mA to reduce charging and result in conductive surfaces (BALTEC SCD 005 Sputter Coater - BALTEC). The pore sizes were measured manually by using ImageJ software.

3.7.2 Field Emission Scanning Electron Microscope

FESEM has a higher resolution in comparison with SEM (around 500 000× magnification). FESEM is used to examine and visualize very small topographic details on the samples surface. Primary electrons are generated from a field emission source accelerated through high vacuum column which are focussed and deflected by electronic lenses to produce a narrow scan beam that bombards the object. Consequently, the secondary electrons will be emitted from each spot on the object. A detector catches the secondary electrons and produces an electronic signal. This signal is amplified and transformed to a video scan-image that can be seen on a monitor or to a digital image that can be saved and processed further. In this research, samples were sputter coated with platinum and underwent FESEM analysis by using JSM-7800F FESEM brand (refer to Appendix 1).

3.7.3 Attenuated Total Reflectance - Fourier Transform Infrared Spectroscopy

ATR-FTIR is a simple technique for examining both solid and liquid samples ATR-FTIR (Perkin Elmer, Spectrum 100, refer to Appendix 1) was used in this study to identify the functional groups and the chemical structures of the samples. Via this technique, the characterization process exhibits the bond present due to either intermolecular or intramolecular interaction in the porous materials, and at a certain peak a reading is formed which indicates to its functional groups such as hydrogen bond, carbonyl bond and ester bond. The peak will be shifted to a different location as

the ratio of the polymer mixture changes. Fourier-transform infrared spectroscopy (FTIR) for scaffolds was performed on Spectrum One (Perkin–Elmer, USA) spectrophotometer over a range of 700 to 4000 cm^{-1} at a resolution of 2 cm^{-1} with 100 scans per sample.

3.7.4   Thermogravimetric Analysis (TGA)

TGA is one of the characterization techniques used to study the behaviour of scaffolds regarding weight loss due to evaporation, decomposition, gas absorption, desorption and dehydration. The mass of the samples must be recorded before this analysis was accomplished and the change in mass can be measured using microbalance. Disturbance on the equilibrium balance beam will change the shutter position, followed by current development in the photodiode resulting from the forthcoming light from the lamp. This imbalance induces a current in the magnetic foil, which generates additional electromagnetic force to recapture equilibrium. As the photodiode current is amplified, the amount of added electromagnetic force is comparative to the mass change. The TGA equipment METTLER Toledo STAR-1 was used in this study (refer to Appendix 1). TGA was carried out by heating 5 mg each of the sample from 50 to 950 °C at a heating rate of 1 °C/min. with nitrogen as purge gas.

3.7.5   Universal Testing Machine

The universal testing machine (refer to Appendix 1) was used to evaluate the mechanical properties of the prepared composite scaffolds; it helps in measuring their extension at break. The normal relation between stress and strain is linear but when the strain is greater than 10%, the curves enters the plastic region; prepared scaffolds were initially measured by dimension width × length: (10 to 12 mm) × (50 to 70 mm) and thickness (8-10 mm). The cut scaffold samples were placed in the universal testing machine (UTM) to test their extension at break.

3.7.6   Swelling behaviour

All scaffolds were cut into 1 cm × 1cm × 1cm and placed in falcon tube. The scaffolds were weighed (W_d) before submerging in PBS. The solution was maintained at

37 °C throughout the analysis. The wet weight of the samples (W_t) was determined after 1, 3 and 7 days by gently blotting them on filter paper. The water uptake or swelling analysis was conducted in triplicates for all types of scaffolds. Swelling ratio was calculated according to Equation 3.1 (Tohamy et al., 2018)

$$\text{Swelling (\%)} = \left(\frac{W_t - W_d}{W_d}\right) \times 100 \text{ \%} \qquad 3.1$$

3.7.7 Porosity

The porosity of the freeze-dried scaffolds was measured using water displacement method. The scaffolds were cut in 1 cm x 1 cm x 1cm sizes and immersed in a known volume (V_1) of water in a Falcon tube for 30 min. The total volume of water and the water impregnated scaffold were recorded as V_2. The water-impregnated scaffolds were then removed from the Falcon tube and the residual water volume was recorded as V_3. Experiments were carried out in six replicates for all types of scaffolds. The porosity of the scaffolds was obtained by Equation 3.2 (Bhardwaj & Kundu, 2011):

$$\text{Porosity (\%)} = \left(\frac{V_1 - V_3}{V_2 - V_3}\right) \times 100 \text{ \%} \qquad 3.2$$

3.7.8 Degradation study

The weight loss percentages were determined after drying the samples in vacuum by comparing the dry weight, W_d at a certain time point with the initial weight, W_0 according to Equation 3.3. The lyophilized scaffolds were cut into 1 cm $\times$ 1cm $\times$ 1cm and placed in Falcon tube containing 3 ml of PBS and incubated at 37 °C. The samples were then taken out at after 7 days. After testing, the scaffolds were washed with distilled water and kept dry in a desiccator for further use.

$$\text{Degradation (\%)} = \left(\frac{W_0 - W_d}{W_0}\right) \times 100 \qquad 3.3$$

3.8 Cell culture studies

In this study, hFOB was utilized to test the biocompatibility of the prepared scaffold. The cell culture studies included MTT assay, cell viability, and cell morphological study.

3.8.1 Cell expansion and seeding

Human fetal osteoblast (hFOB) cells were cultured in DMEM/F-12 medium (1:1) containing 10 % FBS and 1 % cocktail antibiotic in 75 cm² cell culture flasks. The osteoblasts cells were incubated at 37°C in a humidified atmosphere containing 5% CO_2 for 3 days. The cross-linked scaffolds were soaked in 100 % ethanol for 24 h, and then sterilized under UV light for 3 h. These scaffolds were again sterilized with 70 % ethanol for 30 min then washed with PBS for 15 min 3 times and subsequently immersed in cell culture medium overnight. hFOB cells grown in 75 cm² cell culture flasks were detached on confluency by adding 1 ml of 0.25 % trypsin containing 0.1 % EDTA. Detached cells were centrifuged and counted by Trypan blue using haemocytometer, seeded on scaffold at a density of (1×10^4) cells/cm² and incubated to facilitate cell growth.

3.8.2 Cell-scaffold proliferation studies

The proliferation of hFOB cells was quantified using MTT assay; the solution was pipetted into each well of the 96-well assay plate containing the samples in 100 µL of culture medium. The plate was then incubated at 37 °C for 1–4 hours in a humidified 5% CO_2 atmosphere. The amount of soluble formazan produced by cellular reduction of MTT was then measured by immediately recording the absorbance at 490 nm using a 96-well plate reader. The proliferation rate of hFOB cells seeded on prepared scaffold was quantified at 3 and 7 days of culture by performing MTT assay. In this assay, initially, cells were distributed evenly in each well with a size of 1×1 mL in a 12-well cell culture plate (approximate concentration of 5×10^3 cells). The hFOB cells were seeded on prepared scaffolds (n = 4) and left for 1-4 hours of incubation at 37 °C in a humidified, 5% CO_2 atmosphere, where only viable cells lead to the formation of

soluble formazan product. The amount of soluble formazan produced by cellular reduction of MTT was measured by immediately recording the optical density of the samples at 490 nm using a well plate reader. Throughout the whole experiment, the culture medium was replaced regularly with fresh medium in every two days. The absorbance of formazan produced by composite scaffolds was compared with the absorbance of control cultures, where numbers of cells used to seed composite scaffolds and control were in equivalence with scaffold seeding density to finally determine the percentage of cell-seeding efficiency. The cell on well-plate was observed by using inverted microscope.

3.8.3   Cell- scaffold morphological studies

After reaching the specified period, the cells grown on scaffolds were rinsed twice with PBS and fixed in 3 % GA for 60 min. Thereafter, the scaffolds were dehydrated with increasing concentrations of alcohol (20, 40, 60, 80 and 100%) for 10 minute each. The samples were air dried by keeping the samples in a fume hood. Lastly, the scaffolds were sputter coated with platinum and observed using SEM at an accelerating voltage of 10 kV.
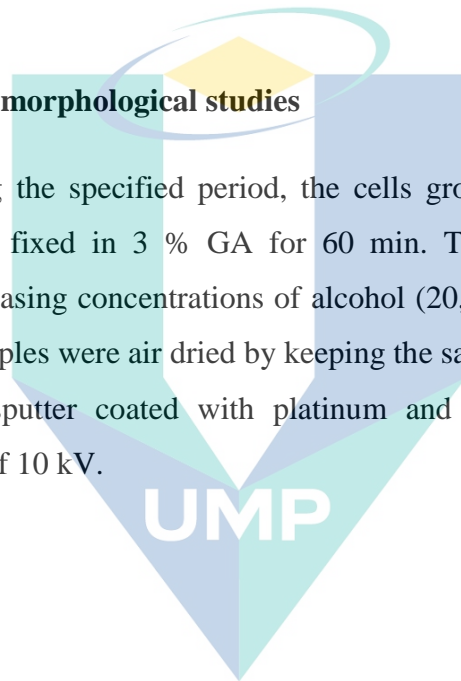
CHAPTER 4

RESULTS AND DISCUSSION

4.1 Introduction

This chapter presented the outcome of the investigations on the production of biopolymeric scaffolds using different combinations of HEC/SA and HEC/SA/CNC, and their treatment with SBF via a freeze-drying technique. Microstructure, morphology, mechanical and thermal properties of the produced scaffolds before and after immersion in simulated bodily fluid was characterized using SEM, ATR-FTIR, TGA and UTM. Other studies include the swelling behaviour, porosity analysis, biodegradability, as well as cell culture investigation of the produced scaffolds.

4.2 Scanning electron microscopy

The surface morphology of scaffolds is one of the crucial factors that influence cell attachment, proliferation and differentiation. Cyster reported a pore size of greater than 100 μm but less than 400 μm is considered to be optimal for osteoconduction for bone in-growth. (Cyster et al., 2005). Similar results have been obtained as shown in Figure 4.1 (a and c), both pure HEC/SA and HEC/SA/CNC exhibited interconnected microstructures with a lamellate shape with diameter in a range of 40 – 400 μm. The structure of the scaffolds mimicked the trabeculae of spongy bone which contains bone cells (such as osteocyte, osteoblast, osteogenic cell, and osteoclast). A study by Woodard et al. (2007) indicated that pore diameters >300 μm can connect tissues such as blood vessels that surrounds bones while 50 μm pore diameters can improve bone regeneration and are advantageous for expanding specific surfaces with increasing amount and variety of cells (Woodard et al., 2007). Novotna et al. (2019) fabricated two types of calcium phosphate scaffolds; one had both macrospores and microspores and the other had only macrospores (Novotna et al., 2019). It was shown that large interconnected macrospores (>300 μm) provided space for bone in-growth,

vascularization, and innervation, while microspores (< 20 μm) improved the capillarity of bone scaffolds which increased the amount and variety of cells drawn through the microporous network. Thus, it is highly favourable to fabricate scaffolds with pore distribution ranging from several micrometres to several hundred micrometres.
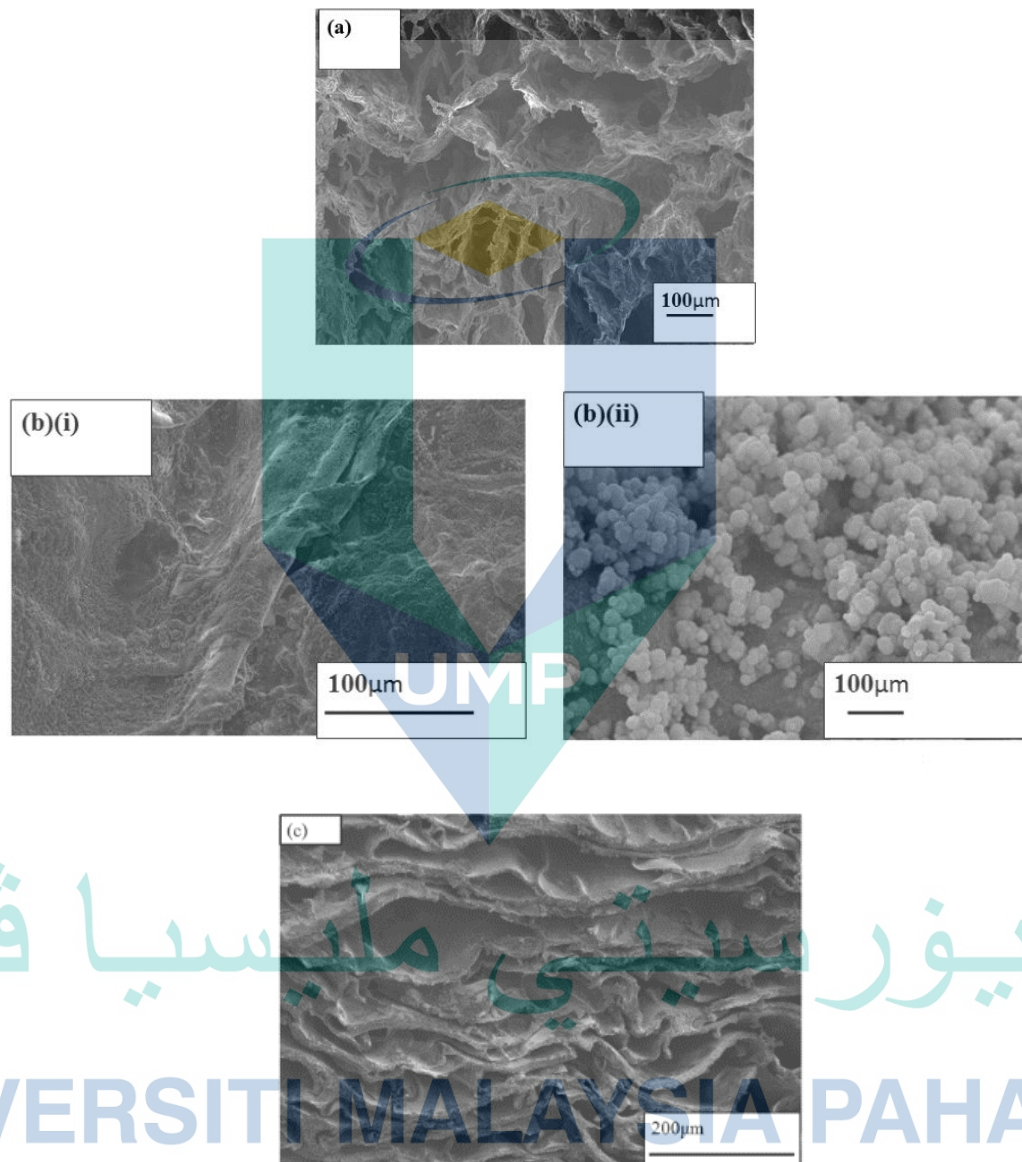
Figure 4.1   SEM images of (a) HEC/SA, (b) HEC/SA (SBF treated) at (i) low magnification and (ii) high magnification, (c) HEC/SA/CNC, (d) HEC/SA/CNC (SBF treated) at (i) low and (ii) high magnification and (e) EDX spectrum for HEC/SA/CNC (treated with SBF
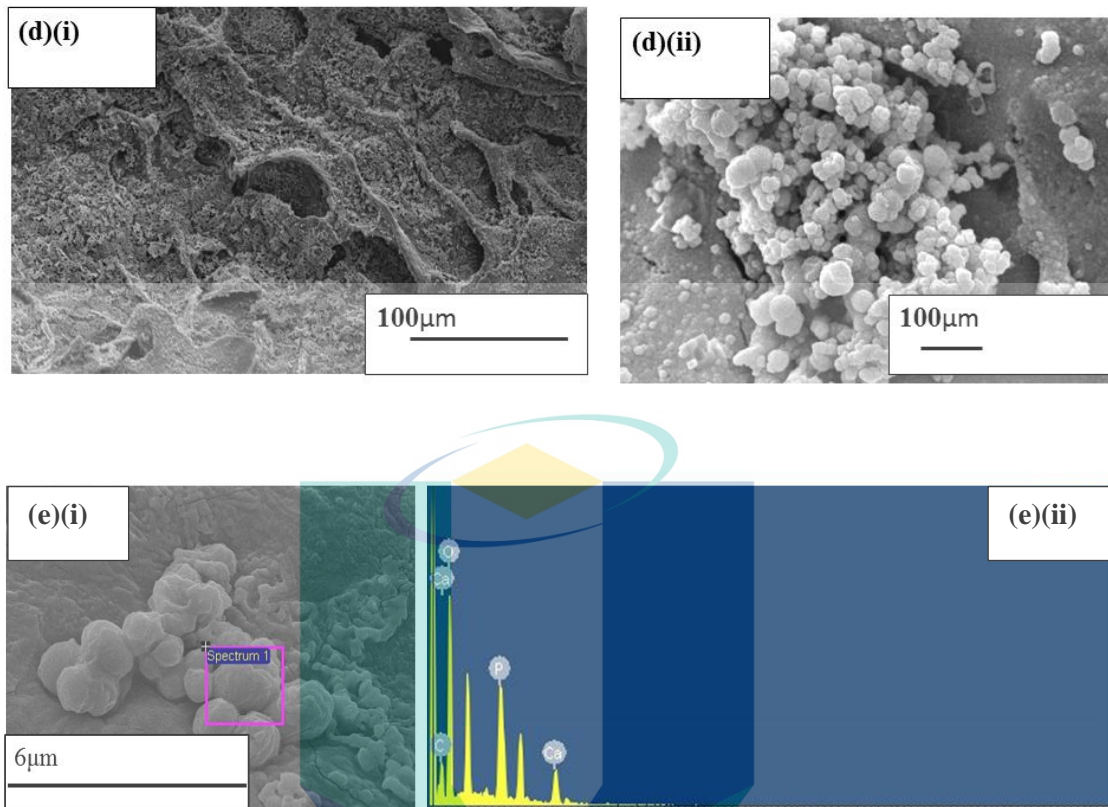
Figure 4.1 Continued

Figure 4.1 (b and d) showed the SEM images after the scaffolds have been immersed in SBF for 24 hours. A sequence of biochemical interactions led to the formation of calcium phosphate or apatite layer on the scaffold surface; this can be attributed to the surface modification during immersion via induction of both Ca^{2+} and PO_4^{3-} ions on the surface of scaffolds (Shin et al 2017). Synthesized scaffolds mineralized with CaP and found that apatite uniformly coated on the scaffold surface, the average particle diameter was measured by image J is 95 nm- 148 nm (refer to Appendix 1), is worth mentioning that these zero-dimensional spherical shape apatite particles increased the surface area of the scaffolds, and provided more osteo-inductive surfaces, along with the formation of new osteoblasts and bone in-growth simultaneously.

Ca-P was predominantly engineered due to its component mimicking the inorganic component of bone. This osteogenic biomolecule could induce osteo-

31

inductivity, and thus promote cell adhesion, proliferation, and differentiation of osteoblasts. Figure 4.1 (e) showed the EDX results for HEC/SA/CNC combination after immersion in SBF for 24 hours. Table 4.1 shows minerals containing 60.35% of calcium and 23.3% of phosphorous. The calcium element is an important element in natural bone due to the greatest effects on formation of bone and osteogenic differentiation (Lei et al., 2017) thus, this proved the appearance of apatite crystals on the scaffolds surface (Henmi et al., 2016).

Table 4.1   Calcium and phosphate percentage

Element	Scaffold HEC/SA co-operated with CNC and treated with SBF
Calcium	60.35%
Phosphorus	23.30%

4.3   Porosity

Porosity is very important for nutrient and oxygen transport from the extracellular matrix to the inner surface of the scaffolds. In comparison of porosity results to Lou study, which used a different layer of SA and polyethylene terephpthate (PET) as bone scaffolds, their work confirmed that porosity slightly decreases when the number of layers decreases (Lou et al., 2015). This was observed in this work based on the percentage porosity for the produced scaffolds shown in Figure 4.3. When comparing the porosity of scaffolds with and without addition of CNC, the pure scaffolds HEC/SA shows porosity at 88.47 % and HEC/SA/CNC shows porosity at 90.13 %, there is only a significant difference in porosity (~1.66 %), this might be due to the presence of CNC that filled the scaffold's pore and permitted the attachment of these zero-dimensional nanoparticles on the scaffold's surface, thereby increasing the volume-to-surface ratio. On the other hand, HEC/SA (SBF) and HEC/SA/CNC(SBF) shows porosity of 77.98% and 75.66 %   respectively, this is due to the bio mineralization process with SBF, which made the scaffolds dense thus reduced the percentages of porosity. Overall, all the scaffolds had sufficient porosity that would support the growth of bone cells through the scaffolds (Tzur-Balter et al., 2013).
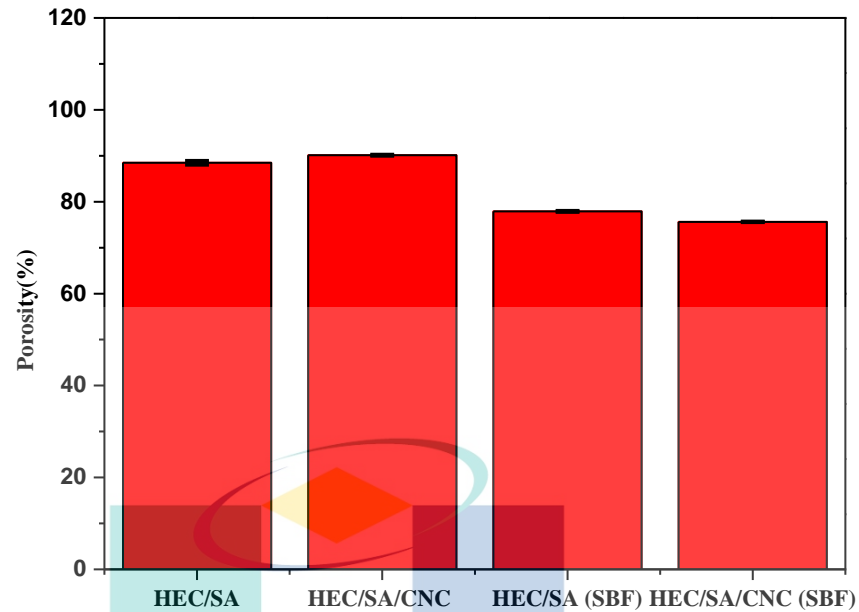
Figure 4.2   Porosity percentage for HEC/SA, HEC/SA/CNC, HEC/SA (SBF) and HEC/SA/CNC (SBF), respectively

4.4   Swelling behavior

The swelling behavior of scaffolds help in the transfer of nutrients and expulsion of wastes out of the scaffolds so as to retain their structure (Siqueira et al., 2019). Swelling is an important feature for bone construction and regeneration in order to maintain its physical structure. In comparison to the study carried out by Zare-Harofteh, which used natural materials (gelatin and akermanite nanocomposite scaffold), scaffolds immersed in distilled water and found that at the beginning, the scaffold absorbed water rapidly and the rate of swelling increased with time. The significant differences in water absorption were not observed when reaching plateau point (Zare-Harofteh et al., 2016) The same observation was noticed in this work. Produced scaffolds showed different swelling behavior as in figure 4.4, where the swelling behavior of HEC/SA scaffold showed the highest water uptake up to ~ 1100 % for a 7 day periods. This was due to nil mediation of SBF and CNC which effects the water absorption of scaffolds. Meanwhile, HEC/SA/CNC (SBF) scaffold shown lowest water uptake ~700 % for 7 days periods. This might be due to the homogenous distribution of Ca-P on the scaffolds surface which caused reduction of the pore sizes and an increased the isotropic properties of the scaffolds. It was also noticeable that all scaffolds showed a higher water uptake with the

33

increment in the number of days due to water absorption which had increased the OH⁻ groups (Qi et al., 2016). Overall, the swelling ratio was found to increase with time on the 1, 3 and 7 days as reported in literature (Siqueira et al., 2019). However, in this case, a controlled swelling ratio could be achieved by introducing the CNC or by SBF immersion, which depends on the behaviour and types of cells and defect tissue.

Figure 4.3   Swelling behaviour for (a) HEC/SA, (b) HEC/SA/CNC, (c) HEC/SA (SBF) and (d) HEC/SA/CNC (SBF) respectively

4.5   Degradation study

The degradation rate of scaffold materials is an essential property for tissue engineering and is of critical importance for the implantation of scaffolds into patients. The degradation was conducted in PBS which is a well-known non-toxic solution specifically used for biological research. It has ionic concentration similar to the human body and acts as a buffer to maintain a constant pH (Nam et al., 2010). The degradation rate of HEC/SA and HEC/SA/CNC scaffolds in PBS at 37 °C over 7 days was assessed as shown in Figure 4.5. After 7 days of incubation, all the scaffolds showed percentage degradation rates of 52.16, 49.16, 46.46 and 40.4% for HEC/SA, HEC/SA/CNC, HEC/SA (SBF treated) and HEC/SA/CNC (SBF treated), respectively. The weight loss decreased with the addition of cellulose nanocrystal and immersion in SBF. Overall, the existence of weight loss might be due to the formation of micro crack within the

scaffold layers which contributed to the disintegration of polymer matrices. The loss of polymer side chain attached to the backbone during immersion in the PBS solution could also impact the material toughness, and thus, breakdown the structure. This experiment revealed the significant role of CNC as filler, as well as the implication of SBF immersion in the present formulation for controlled degradation. A similar study carried out by Zheng on a combination of natural polymers SA/Ca and silk confirmed that composite scaffolds showed good degradability (Zheng et al., 2017) as it is possible to be controlled by regulating through a polymer bio-mineralization process. This was confirmed as the obtained scaffolds showed higher degradation rates compared to that of Zheng and this could be due to the controlled pH used in the produced scaffolds.
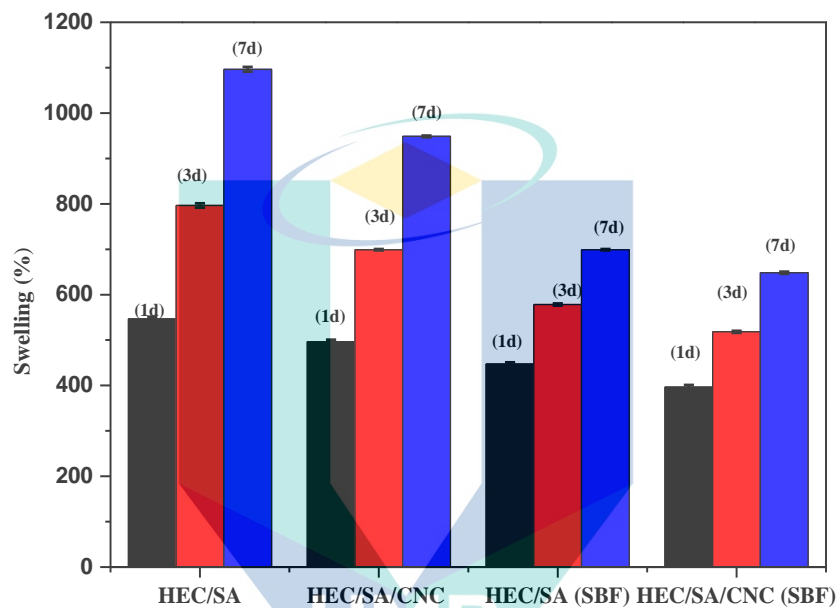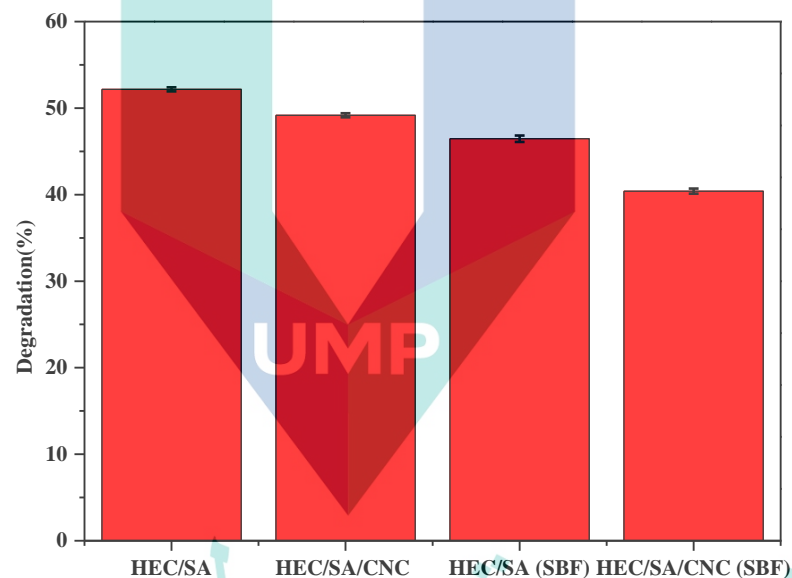

Figure 4.4　　Degradation behaviour for (a) HEC/SA, (b) HEC/SA/CNC, (c) HEC/SA (SBF) and(d) HEC/SA/CNC (SBF) respectively

4.6　　Attenuated total reflectance -Fourier transforms infrared

FTIR spectroscopic technique was used to determine the chemical interaction and bonding between the polymers of the scaffolds. According to a study by Chung which used SA polymer, OH stretched vibration band peaked at 3200 cm^{-1} while aliphatic C-H peaked within the range of 2927-2850 cm^{-1} (Chung et al., 2010). Herein, the ATR-FTIR spectra of the investigated scaffolds, as shown in Figure 4.6, have shown the characteristic O-H bands within the range of 3340 cm^{-1} - 3365 cm^{-1}. However, it is worthy to note that the HEC/SA and HEC/SA/CNC untreated with SBF showed a slight

shift to a lower wave number (3365 cm^{-1}) in comparison to HEC/SA and HEC/SA/CNC scaffolds treated with SBF which were 3340 cm^{-1} and 3359 cm^{-1}, respectively. This could be due to the development interaction scaffolds which possessed higher hydrophilic properties and Ca^{2+} ions reaction with O-H (Corazzari et al., 2015; Kumar et al., 2017). As stated, the greater intensity and shifting of -OH absorption band were evident for the scaffolds without SBF, which suggest that the prepared composite scaffolds showed more hydrophilic behaviour. On the other hand, the peak of C-H group due to the vibrational stretching methylene group shifted to a higher wave number in the produced scaffolds (HEC/SA = 2824 cm^{-1}, HEC/SA/CNC = 2824 cm^{-1}, HEC/SA (SBF) = 2924 cm^{-1}, and HEC/SA/CNC (SBF) = 2873 cm^{-1}). The carbonyl (C=O) group of the scaffolds without immersion in (SBF) peaked at 1628 cm^{-1} due to the bending vibrations of strongly adsorbed water.

The C-O stretching for HEC/SA/CNC (SBF) was observed at 1009 cm^{-1} wavelength and a similar wavelength was found at 1067 cm^{-1} for the other scaffolds. These bands were assigned to the fundamental frequencies of the PO_4^{3-} group. The bands that appeared at 799 and 882 cm^{-1} wavelengths indicated the presence of well crystallized hydroxyapatite contents which also suggested the occurrence of chemical interactions between the scaffold components that ultimately influenced the overall physicochemical, mechanical properties, and *in vitro* bioactivity of the prepared scaffolds (Dogan & Öner, 2008).
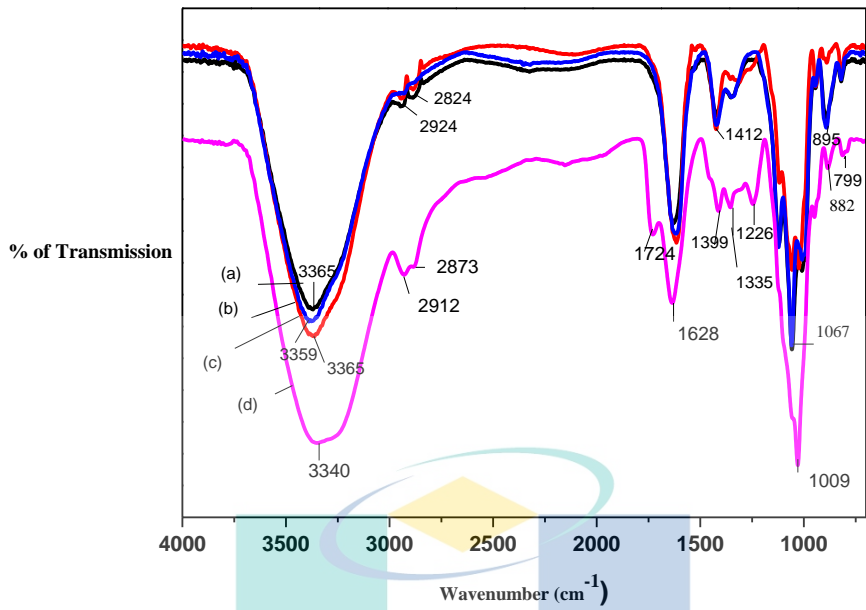
Figure 4.5   FTIR spectra for (a) HEC/SA, (b) HEC/SA/CNC, (c) HEC/SA (SBF) and (d) HEC/SA/CNC (SBF) scaffolds

4.7   Thermogravimetric analysis

TGA was done to investigate the thermal behaviour of the prepared scaffolds. A similar study by Tanan on scaffolds stability used natural polymer and PVA,(Tanan et al., 2019), and confirmed that polymers showed four regions of weight loss; the first weight loss occurs at a temperature range of 25–100°C due to the evaporation of physically weak and chemically strong bound water molecules from the polymer matrix; the second weight loss occurs within the range of 100–240°C due to splitting of starch structure by chain scission, eliminating CO and CO_2; the third weight loss occurs within the temperature range of 250–400°C due to the side chain disintegration of PVA and natural rubber molecules. This study observed similar results as the first region of water loss was attributed to the loss of moisture content within the temperature range of 74°C to 80°C (which corresponded to 5 – 22 % weight loss). It is worth noting that both scaffolds soaked with SBF had low weight losses due to the increase in OH- bonding between HEC and SA towards the apatite group structure. In addition, the CNC free scaffolds which initated the decomposition of water was attributed to the free and bound water molecule from both HEC and SA chemical structures.

In the 2nd region, HEC/SA and HEC/SA/CNC soaked in SBF showed major weight loss at 67% and 45%, respectively, while for both HEC/SA and HEC/SA/CNC scaffolds, the weight loss corresponded to approximately 16 %. This region was attributed to the decomposition of the polysaccharide network due to the breaking of C=C bond in the temperature range of 200°C to 230°C. Further weight loss was observed in the 3rd decomposition region (264°C to 350°C) with a weight loss percentage of up to 32% (more prominent in HEC/SA) which verified the existence of a chemical degradation process resulting from bond scission (carbon-carbon bonds) in the polymeric bone of HEC. A minor weight loss of around 10% was found in scaffolds treated with SBF due to the pyrolysis of calcium alginate and depolymerization of cellulose (Evangelopoulos et al., 2015).

In the final region, the weight loss was ascribed to the dehydroxylation behaviour of calcium phosphate which was associated with up to 10% and 26% for soaked and unsoaked with SBF solutions, respectively as in Table 4.2. The onset temperature for samples with CNC was found to be higher compared to pure HEC/SA

and pure HEC/SA (SBF). However, both samples soaked with SBF exhibited lower thermal stabilities possibly due to the higher crystallinity contributed by the formulation of CNC and HA which produced a higher rate of heat transfer. In addition, the introduction of phosphate groups to CNCs particles during the mineralization step reduced the activation energy for degradation ability due to its lower resistance to pyrolysis (Yildirim & Shaler, 2017). It was also noted that the effects of particle size on both CNC and apatite crystal allowed for the formation of end chains which decomposed at low temperatures. The percentage of the scaffolds containing CNC showed a higher residual rate due to the effects of variables during CNC hydrolysis. Table 4.2 showed the values extracted from the TGA plot in Figure 4.7 (a-d) for the prepared scaffolds.
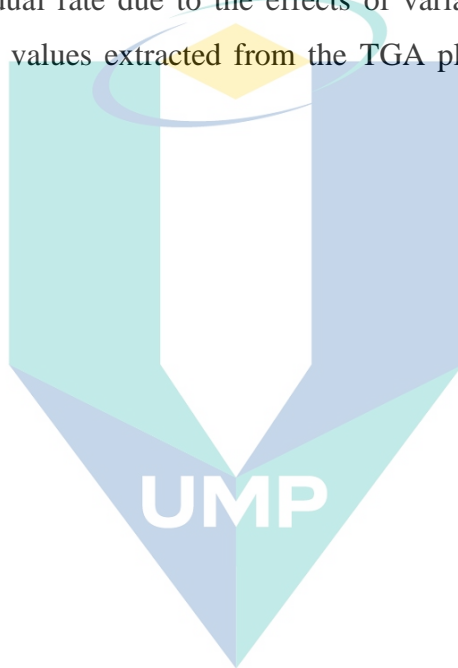
Table 4.2   TGA analysis

Sample	Region of decomposition	Onset temperature (°C)	Weight loss (%) Partial	Total	Residue
HEC/SA	1st	80	22.0		
	2nd	230.49	16.82	86.99	11.99
	3rd	264.03	32.34		
	4th	659.48	15.83		
HEC/SA/CNC	1st	74.4	19.2		
	2nd	234	16	84.2	15.8
	3rd	281	23		
	4th	678	26		
HEC/SA (SBF)	1st	80	5		
	2nd	213	67		
	3rd	330.22	10	87	13
	4th	428	5		
HEC/SA/CNC (SBF)	1st	75	5		
	2nd	200	45		
	3rd	350	14	74	26
	4th	450	10		
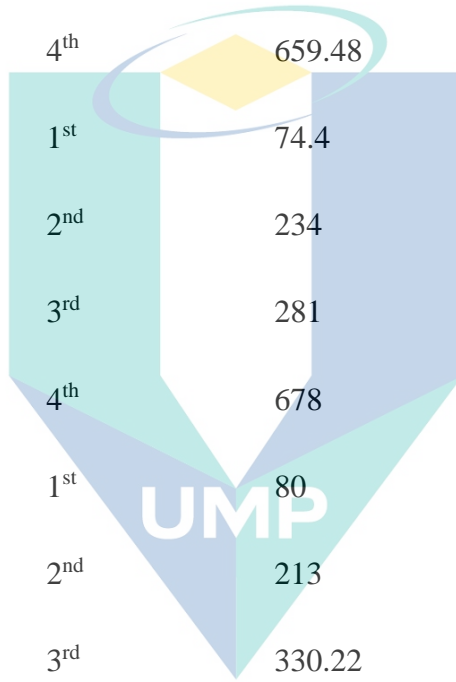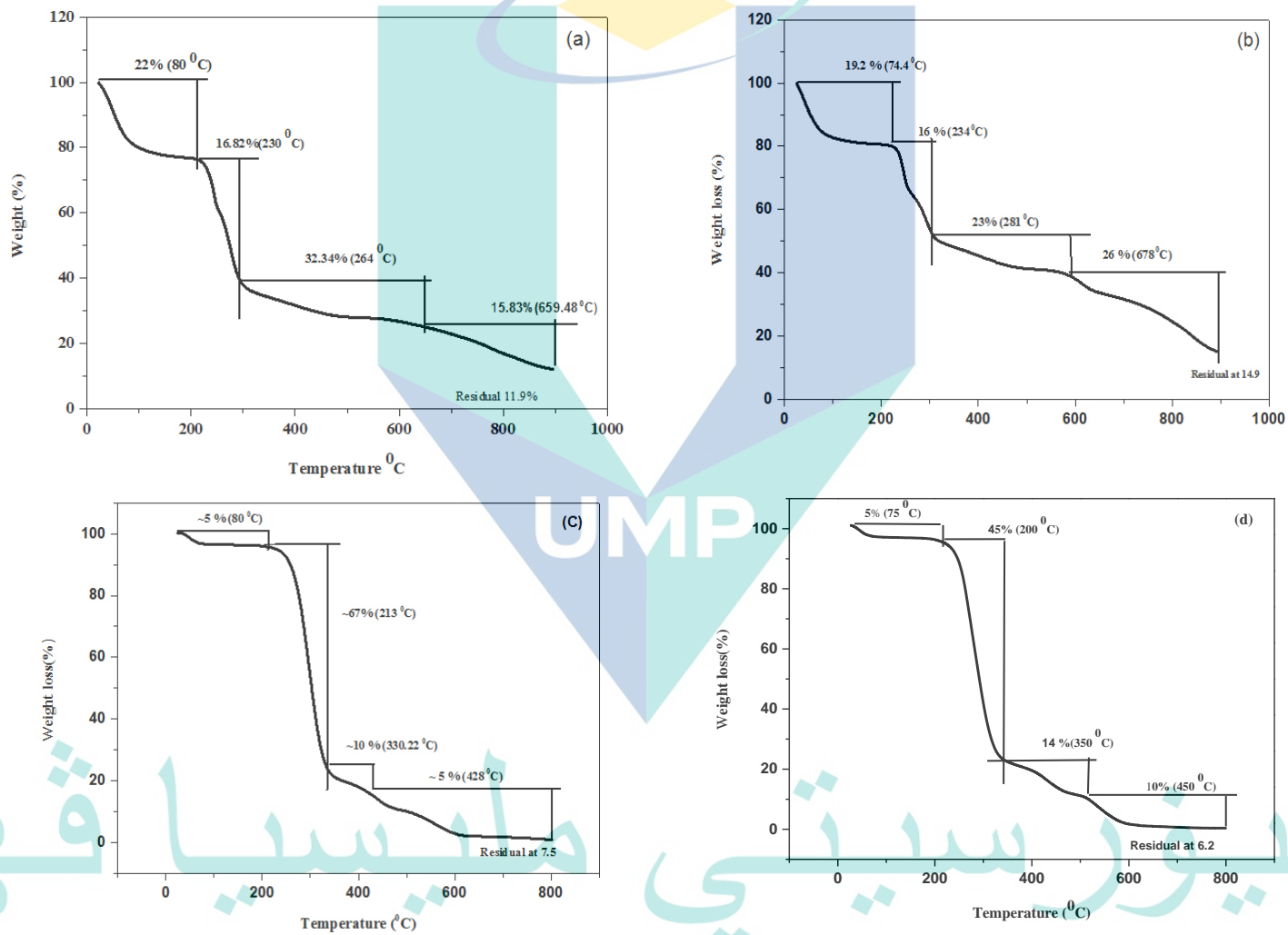
Figure 4.6   TGA graph for (a) HEC/SA, (b) HEC/SA/CNC, (c) HEC/SA (SBF) and (d) HEC/SA/CNC (SBF) scaffolds

4.8 Universal testing machine

Sufficient mechanical strength of composite scaffolds is one of the major prerequisites of an ideal material intended for use in bone tissue engineering (Tohamy et al., 2018). However, one major challenge to researchers is how to obtain a highly porous scaffold with sufficient mechanical strength (Roohani-Esfahani et al., 2016). The range of compressive strength for cancellous bone has been identified as 2-6 MPa (Zare-Harofteh et al., 2016). Stress-strain curves are generally used to evaluate the stress level at varying levels of load or force. Figure 4.8 illustrated the typical non-linear stress-strain curves of all the prepared scaffolds in this study. It is evident that the incorporation of CNC with SBF presented the highest tensile stress (4.15 MPa) in comparison to other scaffolds and this could be due to apatite crystal incorporation into polymeric scaffolds which reduced the pore volume and provided an interface locking that increased the strength of the scaffold.
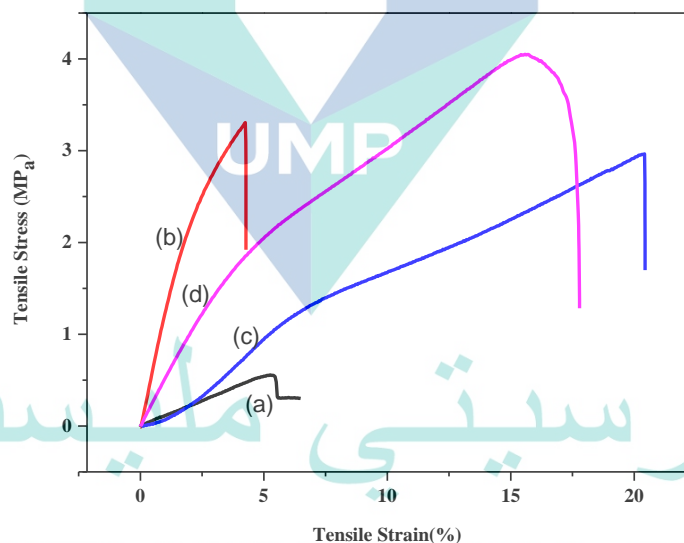
Figure 4.7   Stress-strain graphs for (a) HEC/SA, (b) HEC/SA/CNC, (c) HEC/SA (SBF) and (d) HEC/SA/CNC (SBF) scaffolds

The HEC/SA demonstrated lowest tensile stress and tensile strain values of 0.5 MPa and 5.2%, respectively due to the stress-raiser that easily formed between the pores, making the scaffolds to exhibit brittleness during the testing. HEC/SA/CNC presented the highest tensile stress of 3.48 MPa but exhibited a low tensile strain of 4.75 %, indicating the fragile nature of the scaffolds.

The use of CNC as a filler material which means the composite fiber mats the filler could settle at the inside of the nanofibers and increases the mechanical properties of the scaffolds due to its unique physical properties; meanwhile, lower strain values could be signified by the strong influence of amorphous fractions in HEC (Scaffaro, Lopresti, Botta, Rigogliuso, & Ghersi, 2016). On the other hand, HEC/SA (SBF) showed a high strain value of 20.6 % and a tensile stress value of 3.21 MPa, proving that the immersion in SBF significantly impacted the mechanical properties of the scaffold. The produced scaffolds had compression stress values comparable to those of cancellous bone (range of 2-6 Mpa).

4.9   hFOB cell proliferation and viability

Biopolymeric-based materials are widely used in biomedical implants and devices. Cell-scaffolds surface compatibility is usually investigated by monitoring cell adhesion and proliferation. However, it is difficult to find polymers that meet all the requirements, such as, biocompatibility, bioactivity, hydrophilicity, roughness and mechanical properties. Synthesized polymers normally possess excellent mechanical properties but suffer from insufficient biocompatibility and bioactivity. One possible approach to achieve better biocompatibility is to modify the surface chemical composition of such polymers. In this study, the MTT assay was conducted to assess the biocompatibility of the produced scaffolds.

The principle of the assessment is based on the reduction of tetrazolium compound by enzyme mitochondrial dehydrogenases inside a living cell, thereby leading to the formation of a coloured formazan product which is soluble in cell culture media (Stockert et al., 2012). The concentration of the coloured product helps in estimating the number of metabolically active cells. This test is performed to check the cell viability in an established cell culture line to determine the cell-seeding efficacy along with the cell numbers on seeded scaffolds. MTT assays for different nanocomposite scaffolds containing AL and CNC, were carried out by (Kumar et al., 2017). The scaffolds were incubated for a period of 3 days and cell viability was observed to increase significantly for scaffolds containing CNC in comparison to the scaffolds without CNC. In this study, the MTT assay was carried out for 3 and 7 days

and the proliferation results were shown in Figure 4.9. All the scaffolds showed significant increases in size (p≤ 0.05) from day 3 to day 7 due to the increase in cell attachment and penetration through the porous scaffolds.
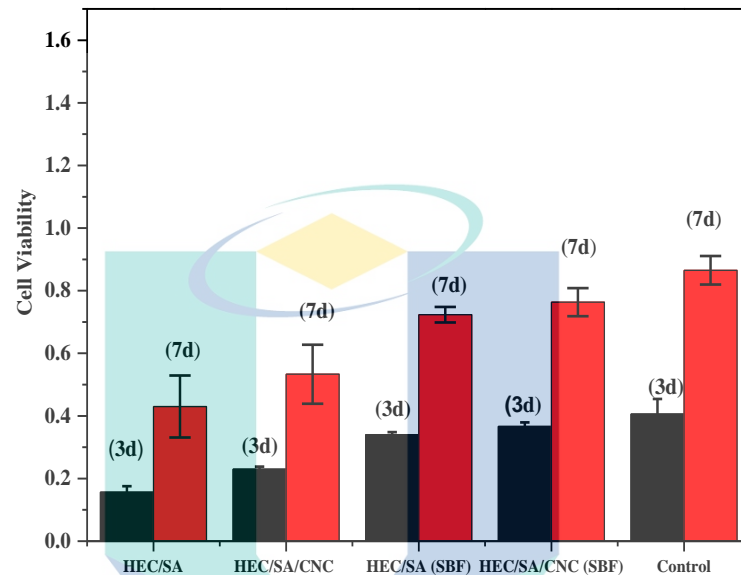
Figure 4.8   MTT assay for 3 and7 days for all scaffolds

On day 3, all the scaffolds presented a positive cell-scaffold interaction with more prominent results observed for HEC/SA/CNC (SBF) scaffold (absorbance index at 0.38). This adhesion and differentiation of hFOB cells might be triggered by the calcium phosphate platform which matched the alkaline phosphatase gene expressed by the cells. Meanwhile, the embedded CNC demonstrated a higher absorbance index due to a higher surface-to-volume ratio that provided more rooms for cells attachment. Furthermore, the pore structure of all the scaffolds showed conducive structure for the cells directly across the pores, as well as those occupying the shallow side of the pores.

The biocompatibility of the cells-scaffold was further confirmed by cells imaging in which the microplate containing the cells was observed via light microscope. The results of the analysed cells indicated that the cells were well attached to the scaffolds, demonstrating major viable cells. The scaffold, (d) HEC/SA/CNC (SBF) showed better results when compared with others scaffold, this is due to less dead cells (dark blue) as in figure 4.11 and displayed the most similar profile with control, the well-plate indicated non-toxicity of the scaffold and a suitable microenvironment that

44

facilitated interaction between the cells, apatite, CNCs and HEC/SA polymer matrices. However, all the produced scaffolds showed growth of bone cells and the growth of bone increased while incubation was increased from 3 to 7 days with minor dead cells (dark blue). A similar study conducted by Tamburaci cultured hFOB cells on the surface of hydrogel and assessed the cells for viability after 7 days (Tamburaci et al., 2018).
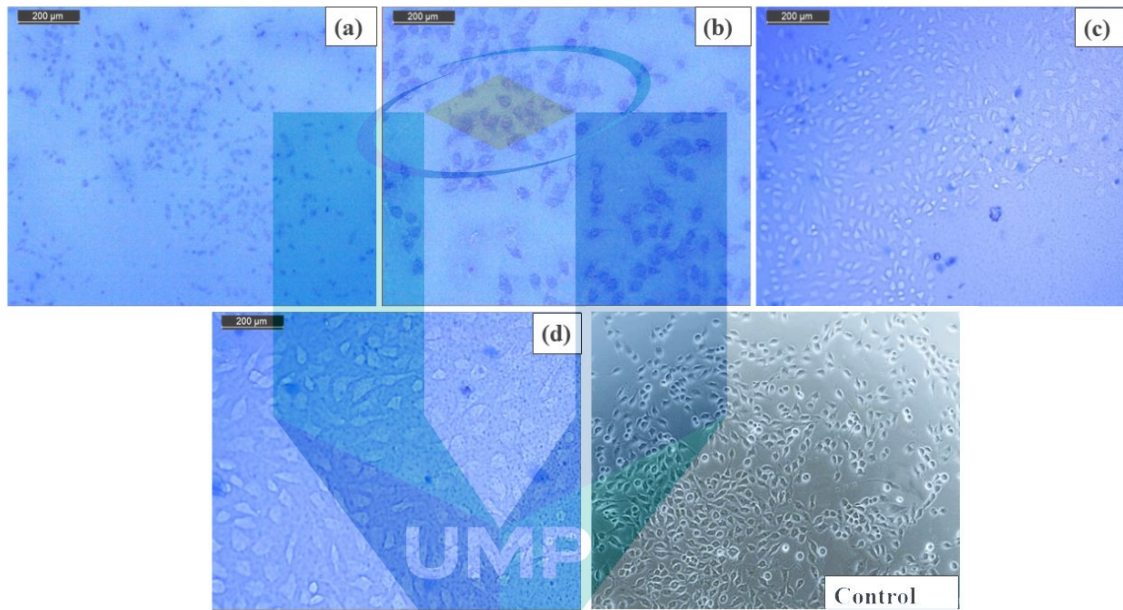
Figure 4.9   Shows SEM micrograph for 3 days incubation for (a) HEC/SA, (b) HEC/SA/CNC, (c) HEC/SA (SBF) and (d) HEC/SA/CNC (SBF) at 400× magnification
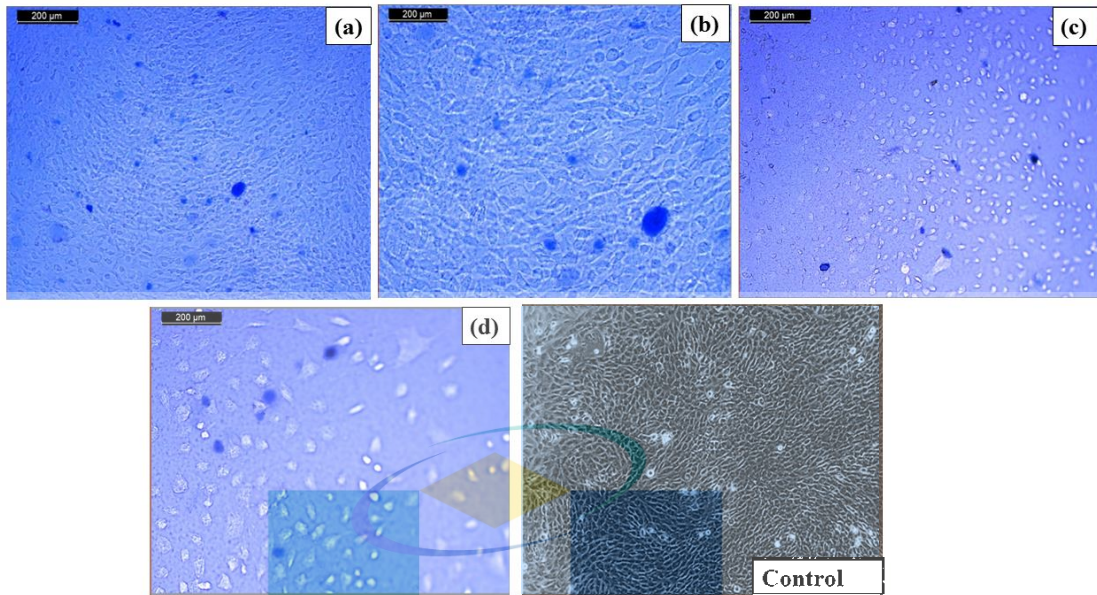
Figure 4.10   Shows SEM micrograph for 7 days incubation for (a) HEC/SA, (b) HEC/SA/CNC, (c) HEC/SA (SBF) and (d) HEC/SA/CNC (SBF) at 400× magnification

4.10   hFOB cell-scaffold morphological studies

Figure 4.12 showed the SEM micrographs of cell-scaffold cultures after 3 and 7 days of culturing at the external and internal surfaces of the scaffolds. After 3 days of cell culturing, the hFOB cells adhered and spread on the scaffolds as shown in Figure 4.12 (a-d). Some confluent layers of osteoblast cells were seen across the valley of the inner surface which formed multiple points of attachments from the surface. The osteoblast cells was observed, indicating that the cell proliferation began to integrate with the rough surface of the scaffolds, implying the inducement of cell attachment. The scaffolds incubated for 3 days and the attached cells were shown in Figure 4.12. Incubation for 7 days shoed more inside and outside layers being covered with cells (see Figure 4.13). The cells were grown in clusters and congregated to form large areas in the culture medium. As a result, the number of osteoblast cells increased with the prolonged time of culturing without any substantial difference between the scaffolds. The favourable environment provided by the scaffolds encouraged cell affinity and cell differentiation. All the scaffolds showed low toxicity and supported the growth of the hFOB cells. According to Tamburaci, hFOB cells that were used on composite scaffolds to test for cell attachment and spreading after seven days of incubation showed attachment and spreading of cells on the surface of the pores on SEM (Tamburaci et al., 2018) and the mineralized scaffold showed poly and flat structures which indicated the

46

initiation of cell differentiation. Similar results were obtained in this study but in comparison to the study by Tamburaci, the prepared scaffolds showed more details of the inside and outside layers.

Figure 4.11   Shows SEM of hFOB cell-scaffold morphological studies for 3days
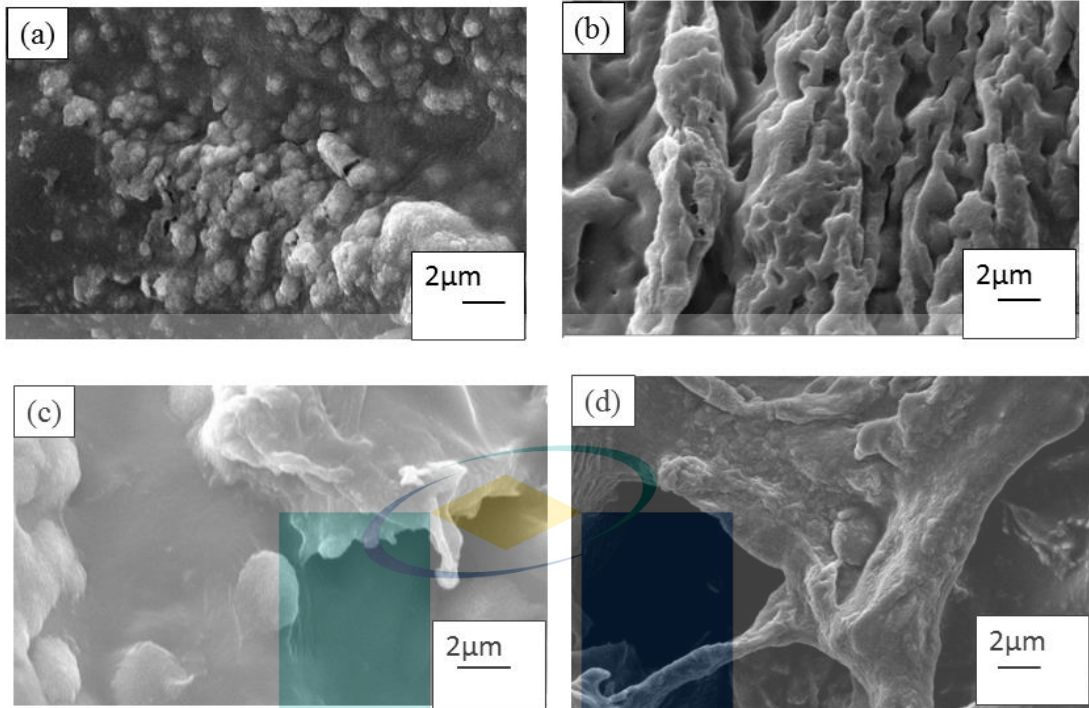
Figure 4.12   Shows SEM of hFOB cell-scaffold morphological studies for 7 days

CHAPTER 5

CONCLUSIONS

5.1   Results Summary

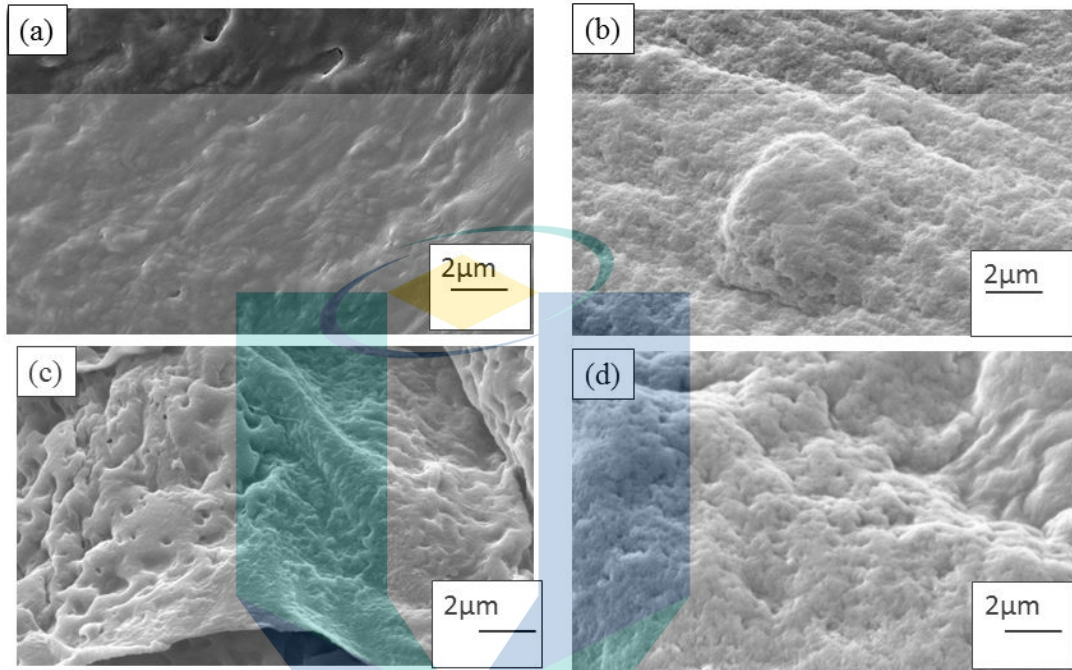This research was conducted to synthesize composite scaffolds using hydroxyl ethyl cellulose (HEC), sodium alginate (SA), and cellulose nanocrystals (CNC) via a freeze-drying method. Scaffolds with different combination as HEC/SA, HEC/SA/CNC, HEC/SA (SBF) and HEC/SA/CNC (SBF) were characterized via scanning electron microscope (SEM), Field emission electron microscopy (FESEM), attenuated total reflectance- (ATR-FTIR), TGA and universal testing machine for mechanical test; also, swelling behaviour, porosity and degradation studies were carried out. Cell culture studies were performed to demonstrate the scaffolds as potential substrates for bone tissue engineering. The SEM images of the scaffolds displayed interconnected porous structures, ranging from 40 to 400 μm. The immersion of scaffolds into SBF deposited apatite layer on the surface of scaffold with the particle size in the range of 95 nm- 148 nm. The porosity of the produced scaffolds was predicted using liquid displacement technique and shown to range from 75 ± 5 % to 90.5 ± 5 %. The swelling behaviour was conducted for the produced scaffolds for 1, 2 and 3 days and the results showed that the scaffolds had the highest swelling behaviour due to absence of cellulose nanocrystals and immersion in SBF. Degradation study was carried out to examine the degradation rate of the scaffolds; this was done by soaking the scaffolds in PBS for two days; HEC/SA/CNC (SBF) scaffolds showed less weight losses in comparison to other produced scaffold.

Meanwhile, ATR-FTIR provided information of chemical bonds, assigning significant fundamental frequencies of the PO_4^{3-} group which appeared at wavelengths 799 and 882 cm⁻¹ and indicated the existence of well crystallized hydroxyapatite contents which also suggests the occurrence of chemical interactions between the scaffolds. The TGA results showed four different regions of mass losses, representing the amorphous transition temperature and water disposal, (C-H) bond breaking,

pyrolysis and dehydroxylation behaviour of hydroxyapatite respectively for each stage. Next, the UTM results revealed that the tensile strength of the produced SA/HEC/CNC (SBF) scaffolds was ~ 4 MPa while the SA/HEC scaffold exhibited tensile stress value of ~ 0.5 MPa which confirmed that the addition of cellulose nanocrystals and immersion in simulated bodily fluid improved the mechanical properties of the scaffolds.

MTT assay was carried out for 3 and 7 days and indicated positive increment of absorbance index cell viability. The micrographs of the produced scaffolds indicated comparable adhesion and interaction between the media and cells-scaffold with the control well plate. Morphological studies conducted on the produced scaffolds, for 3 days incubation, shown multiple points of attachments but for 7 days of incubation there was partial covering of the inside and outside of the cells. Overall, the produced scaffolds (HEC/SA/CNC (SBF)) showed the best results compared to other produced scaffolds in term of porosity (%), swelling behaviour and biodegradation behaviour; they also showed a good cell adhesion and growth during *in* vitro study with human fetal osteoblast cells. The addition of cellulose nanocrystals and immersion in SBF proved to be a better option for synthesizing scaffolds for bone tissue engineering.

5.3   Recommendations for future research

The results of this study are significant and could be of help in the pharmaceutical industry towards the development of new biocompatible scaffolds that would facilitate the healing process of bone tissues. HEC and sodium alginate were used as the main biopolymer and the scaffolds were fabricated via freeze-dried method. The properties of the scaffolds were enhanced by incorporation of cellulose nanocrystals. Cell culture studies demonstrated the potential of the produced scaffolds as substrates for bone tissue engineering.

However, some of the recommendations for future research are as follows:

1.   In this research, only one ceramic phase was used to obtain coating on the surface of synthesized scaffolds; hence, it is recommended to use biphasic ceramic such as SBF and tri-calcium phosphate (TCP) to improve the mechanical properties of the scaffolds.

2. The biodegradability, swelling behaviour, porosity, degradation behaviour, and cell culture experiments were conducted for a period of one to seven days. Computerized methods can be used to reduce experimental trials and optimizing results.
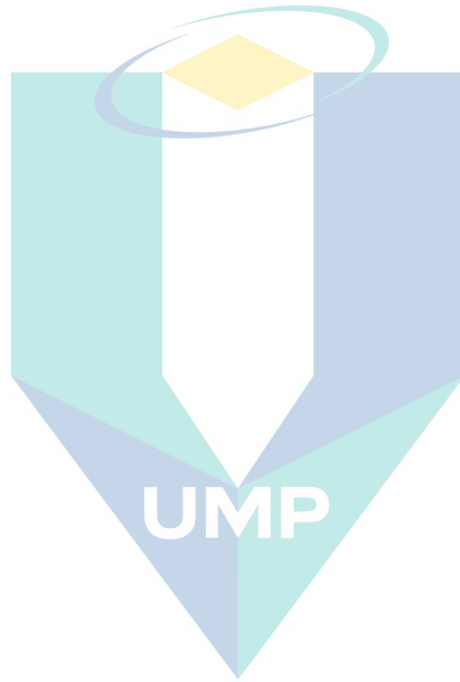
REFERENCES

Affatato, S., Ruggiero, A., & Merola, M. (2015). Advanced biomaterials in hip joint arthroplasty. A review on polymer and ceramics composites as alternative bearings. *Composites Part B: Engineering, 83*, 276-283.

Ahmed, S., & Ikram, S. (2016). Chitosan based scaffolds and their applications in wound healing. *Achievements in the life sciences, 10*(1), 27-37.

Ali, M. E., & Lamprecht, A. (2017). Spray freeze drying as an alternative technique for lyophilization of polymeric and lipid-based nanoparticles. *International Journal of Pharmaceutics, 516*(1-2), 170-177.

Altman, G. H., Diaz, F., Jakuba, C., Calabro, T., Horan, R. L., Chen, J., Lu, H., Richmond, J., & Kaplan, D. L. (2003). Silk-based biomaterials. Biomaterials, 24(3), 401–416. http://www.ncbi.nlm.nih.gov/pubmed/12423595

Agrawal, P., & Pramanik, K. (2019). Enhanced chondrogenic differentiation of human mesenchymal stem cells in silk fibroin/chitosan/glycosaminoglycan scaffolds under dynamic culture condition. *Differentiation*, *110*, 36-48.

Agarwal, S., Wendorff, J. H., & Greiner, A. (2009). Progress in the field of electrospinning for tissue engineering applications. *Advanced Materials, 21*(32-33), 3343-3351.

Barnes, C. (2007). sell sa, Boland eD, simpson DG, Bowlin Gl. nanofiber technology: designing the next generation of tissue engineering scaffolds. *Adv Drug Deliv Rev, 59*(14), 1413-1433.

Bhardwaj, N., Kundu, S.C, (2011), Silk fibroin protein and chitosan polyelectrolyte complex porous scaffolds for tissue engineering applications**. *Carbohydr. Polym.,* 85, pp. 325-333

Brien, F. (2011). Biomaterials & scaffolds Every day thousands of surgical procedures are performed to replace. *Mater Today. Elsevier Ltd, 14*, 88-95.

Catauro, M., Mozzati, M. C., & Bollino, F. (2015). Sol–gel hybrid materials for aerospace applications: Chemical characterization and comparative investigation of the magnetic properties. *Acta Astronautica, 117*, 153-162.

Cen, L., Liu, W. E. I., Cui, L. E. I., Zhang, W., & Cao, Y. (2008). Collagen tissue engineering: development of novel biomaterials and applications. *Pediatric research*, *63*(5), 492-496.

Chan, B., & Leong, K. (2008). Scaffolding in tissue engineering: general approaches and tissue-specific considerations. *European spine journal, 17*(4), 467-479.

Chen, L., Liu, Y., Lai, C., Berry, R., & Tam, K. (2015). Aqueous synthesis and biostabilization of CdS@ ZnS quantum dots for bioimaging applications. Materials Research Express, 2(10), 105401.

Chen, G., Ushida, T., & Tateishi, T. (2002). Scaffold design for tissue engineering. *Macromolecular Bioscience, 2*(2), 67-77.

Chemin, M., Heux, L., Guérin, D., Crowther-Alwyn, L., & Jean, B. (2019). Hybrid Gibbsite Nanoplatelet/Cellulose Nanocrystal Multilayered Coatings for Oxygen Barrier Improvement. *Frontiers in Chemistry, 7*(507). doi: 10.3389/fchem.2019.00507

Chiaoprakobkij,N.,Sanchavanakit,N.,Subbalekha,K.,Pavasant,P.,&Phisalaphong,M (2011).Characterization and biocompatibility of bacterial cellulose/alginate composite sponge with human keratinocytes and gingival fibroblasts. *Carbohydrate Polymers*, 85, 548–553.

Chinnappan, A., Lee, J. K. Y., Jayathilaka, W., & Ramakrishna, S. (2018). Fabrication of MWCNT/Cu nanofibers via electrospinning method and analysis of their electrical conductivity by four-probe method. *International Journal of Hydrogen Energy, 43*(2), 721-729.

Chung, S., Ingle, N.P., Montero, G.A., Kim, S.H., King, M.W. (2010). Bioresorbable elastomeric vascular tissue engineering scaffolds via melt spinning and electrospinning. *Acta Biomater*, 6, 1958–1967.

Cooper, L. N., & Maas, M. C. (2018). Bones and teeth, histology of *Encyclopedia of Marine Mammals* (pp. 114-118): Elsevier.

Corazzari, I., Nisticò, R., Turci, F., Faga, M. G., Franzoso, F., Tabasso, S., & Magnacca, G. (2015). Advanced physico-chemical characterization of chitosan by means of TGA coupled on-line with FTIR and GCMS: Thermal degradation and water adsorption capacity. *Polymer Degradation and Stability, 112*, 1-9.

Cox, S. C., Thornby, J. A., Gibbons, G. J., Williams, M. A., & Mallick, K. K. (2015). 3D printing of porous hydroxyapatite scaffolds intended for use in bone tissue engineering applications. *Materials Science and Engineering: C, 47*, 237-247.

Cyster, L. A., Grant, D. M., Howdle, S. M., Rose, F. R. A. J., Irvine, D. J., Freeman, D., ... & Shakesheff, K. M. (2005). The influence of dispersant concentration on the pore morphology of hydroxyapatite ceramics for bone tissue engineering. *Biomaterials*, *26*(7), 697-702

De France, K.J. , Chan K.J.W. , Cranston E.D. Cranston, Hoare T. (2016), Enhanced mechanical properties in cellulose nanocrystal-poly(oligoethylene glycol methacrylate) injectable nanocomposite hydrogels through control of physical and chemical cross-linking *Biomacromolecules,* 17 (2) pp. 649-660

Deluzio, T. G., Seifu, D. G., & Mequanint, K. (2013). 3D scaffolds in tissue engineering and regenerative medicine: beyond structural templates? *Pharmaceutical Bioprocessing, 1*(3), 267-281.

Dogan, Ö., & Öner, M. (2008). The influence of polymer architecture on nanosized hydroxyapatite precipitation. *Journal of nanoscience and nanotechnology, 8*(2), 667-674.

Evangelopoulos, P., Kantarelis, E., & Yang, W. (2015). Investigation of the thermal decomposition of printed circuit boards (PCBs) via thermogravimetric analysis (TGA) and analytical pyrolysis (Py–GC/MS). *Journal of Analytical and Applied Pyrolysis, 115*, 337-343.

Geng, F., Tan, L., Zhang, B., Wu, C., He, Y., Yang, J., & Yang, K. (2009). Study on β-TCP coated porous Mg as a bone tissue engineering scaffold material. *Journal of Materials Sciences and Technology, 25*(01), 123-129.

George, J., & Sabapathi, S. N. (2015). Cellulose nanocrystals: Synthesis, functional properties, and applications. Nanotechnology, Science and Applications, 8. https://doi.org/10.2147/NSA.S64386

Ghaee, A., Nourmohammadi, J., & Danesh, P. (2017). Novel chitosan-sulfonated chitosan-polycaprolactone-calcium phosphate nanocomposite scaffold. *Carbohydrate polymers*, *157*, 695-703.

Gómez, S., Vlad, M., López, J., & Fernández, E. (2016). Design and properties of 3D scaffolds for bone tissue engineering. *Acta Biomaterialia, 42*, 341-350.

Goonoo, N., Bhaw-Luximon, A., Bowlin, G. L., & Jhurry, D. (2013). An assessment of biopolymer-and synthetic polymer-based scaffolds for bone and vascular tissue engineering. *Polymer International*, *62*(4), 523-533.

Grishkewich, N., Mohammed, N., Tang, J., & Tam, K. C. (2017). Recent advances in the application of cellulose nanocrystals. Current Opinion in Colloid & Interface Science, 29, 32–45. https://doi.org/10.1016/J.COCIS.2017.01.005

Hakkou, K., Molina-Pinilla, I., Rangel-Núñez, C., Suárez-Cruz, A., Pajuelo, E., & Bueno-Martínez, M. (2019). Synthesis of novel (bio) degradable linear azo polymers conjugated with olsalazine. *Polymer Degradation and Stability, 167*, 302-312.

Han, S., Lee, H., Hong, I., Kim, U., & Lee, S. (2017). Non-structural cancellous bone graft and headless compression screw fixation for treatment of scaphoid waist non-union. *Orthopaedics & Traumatology: Surgery & Research, 103*(1), 89-93.

Henmi, A., Okata, H., Anada, T., Yoshinari, M., Mikami, Y., Suzuki, O., & Sasano, Y. (2016). Bone matrix calcification during embryonic and postembryonic rat calvarial development assessed by sem–edx spectroscopy, xrd, and ftir spectroscopy. *Journal of bone and mineral metabolism, 34*(1), 41-50.

Heydarkhan-Hagvall, S., Schenke-Layland, K., Dhanasopon, A. P., Rofail, F., Smith, H., Wu, B. M., ... & MacLellan, W. R. (2008). Three-dimensional electrospun ECM-based hybrid scaffolds for cardiovascular tissue engineering. *Biomaterials*, *29*(19), 2907-2914.

Hopkins, S., Toms, A., Brown, M., Welsman, J., Ukoumunne, O., & Knapp, K. (2016). A study investigating short-and medium-term effects on function, bone mineral density and lean tissue mass post-total knee replacement in a Caucasian female post-menopausal population: implications for hip fracture risk. *Osteoporosis International, 27*(8), 2567-2576.

Hutmacher, D. W. (2000). Scaffolds in tissue engineering bone and cartilage. Biomaterials, 21(24), 2529–2543. http://www.ncbi.nlm.nih.gov/pubmed/11071603

Kanungo, B. P., Silva, E., Van Vliet, K., & Gibson, L. J. (2008). Characterization of mineralized collagen–glycosaminoglycan scaffolds for bone regeneration. *Acta biomaterialia*, *4*(3), 490-503.

Kokubo, T., Kushitani, H., Sakka, S., Kitsugi,T., & Yamamuro, T (1990).Solutions able to reproduce in vivo surface-structure changes in bioactive glass-ceramic A-W, *J. Biomed. Mater. Res.,* 24, 721-734

Kong, L., Gao, Y., Lu, G., Gong, Y., Zhao, N., & Zhang, X. (2006). A study on the bioactivity of chitosan/nano-hydroxyapatite composite scaffolds for bone tissue engineering. *European Polymer Journal, 42*(12), 3171-3179.

Kumar, A., Rao, K. M., & Han, S. S. (2017). Development of sodium alginate-xanthan gum based nanocomposite scaffolds reinforced with cellulose nanocrystals and halloysite nanotubes. *Polymer Testing*, *63*, 214-225.

Kumar, A., Lee, Y., Kim, D., Rao, K. M., Kim, J., Park, S., . . . Han, S. S. (2017). Effect of crosslinking functionality on microstructure, mechanical properties, and in vitro cytocompatibility of cellulose nanocrystals reinforced poly (vinyl alcohol)/sodium alginate hybrid scaffolds. *International journal of biological macromolecules, 95*, 962-973.

Langer, R., Vacanti, J.P. (1993). Tissue engineering. *Science, 260*, 920–926

Lee, S. H., & Shin, H. (2007). Matrices and scaffolds for delivery of bioactive molecules in bone and cartilage tissue engineering. Advanced drug delivery reviews, 59(4-5), 339-359.

Lee, Y. B., Song, S.-J., Shin, Y. C., Jung, Y. J., Kim, B., Kang, M. S., . . . Jung, S.-H. (2019). Ternary nanofiber matrices composed of PCL/black phosphorus/collagen to enhance osteodifferentiation. *Journal of Industrial and Engineering Chemistry*.

Lei, Y., Xu, Z., Ke, Q., Yin, W., Chen, Y., Zhang, C., & Guo, Y. (2017). Strontium hydroxyapatite/chitosan nanohybrid scaffolds with enhanced osteoinductivity for bone tissue engineering. *Materials Science and Engineering: C, 72*, 134-142.

Leukers, B., Gülkan, H., Irsen, S. H., Milz, S., Tille, C., Schieker, M., & Seitz, H. (2005). Hydroxyapatite scaffolds for bone tissue engineering made by 3D printing. *Journal of Materials Science: Materials in Medicine, 16*(12), 1121-1124.

Liao, S., Murugan, R., Chan, C. K., & Ramakrishna, S. (2008). Processing nanoengineered scaffolds through electrospinning and mineralization suitable for biomimetic bone tissue engineering. *Journal of the mechanical behavior of biomedical materials*, *1*(3), 252-260.

Li, M., Yang, X., Wang, W., Zhang, Y., Wan, P., Yang, K., & Han, Y. (2017). Evaluation of the osteo-inductive potential of hollow three-dimensional magnesium-strontium substitutes for the bone grafting application. *Materials Science and Engineering: C, 73*, 347-356.

Li, Y., Jia, H., Pan, F., Jiang, Z., & Cheng, Q. (2012). Enhanced anti-swelling property and dehumidification performance by sodium alginate–poly(vinyl alcohol)/polysulfone composite hollow fiber membranes. Journal of Membrane Science, 407–408, 211–220. https://doi.org/10.1016/j.memsci.2012.03.049

Lou, C. W., Huang, C. L., Chen, C. K., Liu, C. F., Wen, S. P., & Lin, J. H. (2015). Effect of different manufacturing methods on the conflict between porosity and mechanical properties of spiral and porous polyethylene terephthalate/sodium alginate bone scaffolds. *Materials*, *8*(12), 8768-8779

Lu, T., Li, Y., & Chen, T. (2013). Techniques for fabrication and construction of three-dimensional scaffolds for tissue engineering. International Journal of Nanomedicine, 8, 337–350. https://doi.org/10.2147/IJN.S38635

Liu, J., Ruan, J., Chang, L., Yang, H., & Ruan, W. (2017). Porous Nb-Ti-Ta alloy scaffolds for bone tissue engineering: Fabrication, mechanical properties and in vitro/vivo biocompatibility. *Materials Science and Engineering: C*, *78*, 503-512.

Limongi, T., Lizzul, L., Giugni, A., Tirinato, L., Pagliari, F., Tan, H., . . . Brusatin, G. (2017). Laboratory injection molder for the fabrication of polymeric porous poly-epsilon-caprolactone scaffolds for preliminary mesenchymal stem cells tissue engineering applications. *Microelectronic Engineering, 175*, 12-16.

Liu, W., Wang, D., Huang, J., Wei, Y., Xiong, J., Zhu, W., . . . Wang, D. (2017). Low-temperature deposition manufacturing: A novel and promising rapid prototyping technology for the fabrication of tissue-engineered scaffold. *Materials Science and Engineering: C, 70*, 976-982.

Lu, J. W., Zhu, Y. L., Guo, Z. X., Hu, P., & Yu, J. (2006). Electrospinning of sodium alginate with poly (ethylene oxide). *Polymer*, *47*(23), 8026-8031.

Martin, T. J., & Sims, N. A. (2015). RANKL/OPG; Critical role in bone physiology. *Reviews in Endocrine and Metabolic Disorders, 16*(2), 131-139.

Martin, V., & Bettencourt, A. (2018). Bone regeneration: Biomaterials as local delivery systems with improved osteoinductive properties. *Materials Science and Engineering: C*, *82*, 363-371.

Martin, V., & Bettencourt, A. (2018). Bone regeneration: Biomaterials as local delivery systems with improved osteoinductive properties. *Materials Science and Engineering: C, 82*, 363-371.

Martins, A., Araújo, J. V., Reis, R. L., & Neves, N. M. (2007). Electrospun nanostructured scaffolds for tissue engineering applications.

Meryman, H. T. (1976). Historical recollections of freeze-drying. Developments in Biological Standardization, 36, 29–32. http://www.ncbi.nlm.nih.gov/pubmed/801137

Miranda-Nieves, D., & Chaikof, E. L. (2016). Collagen and elastin biomaterials for the fabrication of engineered living tissues. *ACS Biomaterials Science & Engineering, 3*(5), 694-711.

Nam, J.-Y., Kim, H.-W., Lim, K.-H., Shin, H.-S., & Logan, B. E. (2010). Variation of power generation at different buffer types and conductivities in single chamber microbial fuel cells. *Biosensors and Bioelectronics, 25*(5), 1155-1159.

Ngiam, M., Liao, S., Patil, A. J., Cheng, Z., Chan, C. K., & Ramakrishna, S. (2009). The fabrication of nano-hydroxyapatite on PLGA and PLGA/collagen nanofibrous composite scaffolds and their effects in osteoblastic behavior for bone tissue engineering. *Bone*, *45*(1), 4-16.

Novotna, L., Kucera, L., Hampl, A., Drdlik, D., Cihlar Jr, J., & Cihlar, J. (2019). Biphasic calcium phosphate scaffolds with controlled pore size distribution prepared by in-situ foaming. *Materials Science and Engineering: C*, *95*, 363-370.

Pangon, A., Saesoo, S., Saengkrit, N., Ruktanonchai, U., & Intasanta, V. (2016). Hydroxyapatite-hybridized chitosan/chitin whisker bionanocomposite fibers for bone tissue engineering applications. Carbohydrate polymers, 144, 419-427.

Peresin, M. S., Habibi, Y., Zoppe, J. O., Pawlak, J. J., & Rojas, O. J. (2010). Nanofiber composites of polyvinyl alcohol and cellulose nanocrystals: manufacture and characterization. Biomacromolecules, 11(3), 674–681. https://doi.org/10.1021/bm901254n

Porter, J. R., Henson, A., & Popat, K. C. (2009). Biodegradable poly (ε-caprolactone) nanowires for bone tissue engineering applications. *Biomaterials*, *30*(5), 780-788.

Pourasghar, M., Koenneke, A., Meiers, P., & Schneider, M. (2019). Development of a fast and precise method for simultaneous quantification of the PLGA monomers lactic and glycolic acid by HPLC. *Journal of pharmaceutical analysis, 9*(2), 100-107.

Qi, H., Ye, Z., Ren, H., Chen, N., Zeng, Q., Wu, X., & Lu, T. (2016). Bioactivity assessment of PLLA/PCL/HAP electrospun nanofibrous scaffolds for bone tissue engineering. *Life Sciences, 148*, 139-144. doi: https://doi.org/10.1016/j.lfs.2016.02.040

Ramakrishna, S., Ramalingam, M., Kumar, T. S., & Soboyejo, W. O. (2016). *Biomaterials: a nano approach*: CRC press.

Ren, H., Yu, Y., & An, T. (2020). Bioaccessibilities of metal (loid) s and organic contaminants in particulates measured in simulated human lung fluids: A critical review. *Environmental Pollution*, 115070.

Rezaei, A., & Mohammadi, M. (2013). In vitro study of hydroxyapatite/polycaprolactone (HA/PCL) nanocomposite synthesized by an in situ sol–gel process. *Materials Science and Engineering: C, 33*(1), 390-396.

Ribeiro, C., Sencadas, V., Correia, D. M., & Lanceros-Méndez, S. (2015). Piezoelectric polymers as biomaterials for tissue engineering applications. *Colloids and Surfaces B: Biointerfaces, 136*, 46-55.

Rodrigues, M. T., Gomes, M. E., & Reis, R. L. (2011). Current strategies for osteochondral regeneration: from stem cells to pre-clinical approaches. *Current opinion in biotechnology*, *22*(5), 726-733.

Roohani-Esfahani, S.-I., Newman, P., & Zreiqat, H. (2016). Design and fabrication of 3D printed scaffolds with a mechanical strength comparable to cortical bone to repair large bone defects. *Scientific reports, 6*, 19468.

Sanchez, C., Mazzucchelli, G., Lambert, C., Comblain, F., DePauw, E., & Henrotin, Y. (2018). Proteomic analysis of osteoblasts secretome provides new insights in mechanisms underlying osteoarthritis subchondral bone sclerosis. *Osteoarthritis and Cartilage, 26*, S89.

Saha, N., Shah, R., Gupta, P., Mandal, B. B., Alexandrova, R., Sikiric, M. D., & Saha, P. (2019). PVP-CMC hydrogel: An excellent bioinspired and biocompatible scaffold for osseointegration. *Materials Science and Engineering: C*, *95*, 440-449.

Scaffaro, R., Lopresti, F., Botta, L., Rigogliuso, S., & Ghersi, G. (2016). Preparation of three-layered porous PLA/PEG scaffold: relationship between morphology, mechanical behavior and cell permeability. *Journal of the mechanical behavior of biomedical materials, 54*, 8-20.

Schoof, H., Apel, J., Heschel, I., & Rau, G. (2001). Control of pore structure and size in freeze-dried collagen sponges. Journal of Biomedical Materials Research, 58(4), 352–357. http://www.ncbi.nlm.nih.gov/pubmed/11410892

Shaabani, A., Hezarkhani, Z., & Badali, E. (2016). Natural silk supported manganese dioxide nanostructures: synthesis and catalytic activity in aerobic oxidation and one-pot tandem oxidative synthesis of organic compounds. *Polyhedron, 107*, 176-182.

Sheehy, E. J., Vinardell, T., Toner, M. E., Buckley, C. T., & Kelly, D. J. (2014). Altering the architecture of tissue engineered hypertrophic cartilaginous grafts facilitates vascularisation and accelerates mineralisation. *PloS one*, *9*(3), e90716.

Shin, K., Acri, T., Geary, S., & Salem, A. K. (2017). Biomimetic mineralization of biomaterials using simulated body fluids for bone tissue Engineering and regenerative medicine. *Tissue Engineering Part A, 23*(19-20), 1169-1180.

Siqueira, P., Siqueira, É., De Lima, A. E., Siqueira, G., Pinzón-Garcia, A. D., Lopes, A. P., . . . Botaro, V. R. (2019). Three-Dimensional Stable Alginate-Nanocellulose Gels for Biomedical Applications: Towards Tunable Mechanical Properties and Cell Growing. *Nanomaterials, 9*(1), 78.

Stratton, S., Shelke, N. B., Hoshino, K., Rudraiah, S., & Kumbar, S. G. (2016). Bioactive polymeric scaffolds for tissue engineering. *Bioactive Materials, 1*(2), 93-108.

Stockert, J. C., Blázquez-Castro, A., Cañete, M., Horobin, R. W., & Villanueva, Á. (2012). MTT assay for cell viability: Intracellular localization of the formazan product is in lipid droplets. *Acta histochemica, 114*(8), 785-796

Subia, B., Kundu, J., & Kundu, S. C. (2010). Biomaterial scaffold fabrication techniques for potential tissue engineering applications. In D. Eberli (Ed.), Tissue engineering (Issue 3, pp. 141–159). InTech.

Sundberg, J., Götherström, C., & Gatenholm, P. (2015). Biosynthesis and in vitro evaluation of macroporous mineralized bacterial nanocellulose scaffolds for bone tissue engineering. *Bio-medical materials and engineering, 25*(1), 39-52.

Tamburaci, S., & Tihminlioglu, F. (2018). Biosilica incorporated 3D porous scaffolds for bone tissue engineering applications. *Materials Science and Engineering: C*, *91*, 274-291.

Tang, T., Ebacher, V., Cripton, P., Guy, P., McKay, H., & Wang, R. (2015). Shear deformation and fracture of human cortical bone. *Bone, 71*, 25-35.

Tang, J., Sisler, J., Grishkewich, N., & Tam, K. C. (2017). Functionalization of cellulose nanocrystals for advanced applications. Journal of Colloid and Interface Science, 494, 397–409. https://doi.org/10.1016/j.jcis.2017.01.077

Tanan, W., Panichpakdee, J., & Saengsuwan, S. (2019). Novel biodegradable hydrogel based on natural polymers: Synthesis, characterization, swelling/reswelling and biodegradability. *European Polymer Journal*, *112*, 678-687.

Tohamy, K. M., Mabrouk, M., Soliman, I. E., Beherei, H. H., & Aboelnasr, M. A. (2018). Novel alginate/hydroxyethyl cellulose/hydroxyapatite composite scaffold for bone regeneration: In vitro cell viability and proliferation of human mesenchymal stem cells. *International journal of biological macromolecules, 112*, 448-460.

Tomlinson, D., Erskine, R., Morse, C., Winwood, K., & Onambélé-Pearson, G. (2016). The impact of obesity on skeletal muscle strength and structure through adolescence to old age. *Biogerontology, 17*(3), 467-483.

Tuzlakoglu, K., Bolgen, N., Salgado, A. J., Gomes, M. E., Piskin, E., & Reis, R. L. (2005). Nano-and micro-fiber combined scaffolds: a new architecture for bone tissue engineering. *journal of materials science: materials in medicine*, *16*(12), 1099-1104.

Tzur-Balter, A., Gilert, A., Massad-Ivanir, N., & Segal, E. (2013). Engineering porous silicon nanostructures as tunable carriers for mitoxantrone dihydrochloride. *Acta Biomaterialia, 9*(4), 6208-6217

Venugopal, J., Low, S., Choon, A. T., Kumar, T. S., & Ramakrishna, S. (2008). Mineralization of osteoblasts with electrospun collagen/hydroxyapatite nanofibers. *Journal of Materials Science: Materials in Medicine*, *19*(5), 2039-2046.

Vepari, C., & Kaplan, D. L. (2007). Silk as a Biomaterial. Progress in Polymer Science, 32(8–9), 991–1007. https://doi.org/10.1016/j.progpolymsci.2007.05.013

Vig, K., Chaudhari, A., Tripathi, S., Dixit, S., Sahu, R., Pillai, S., . . . Singh, S. R. (2017). Advances in skin regeneration using tissue engineering. *International journal of molecular sciences, 18*(4), 789.

Vrana, N. E. (2016). Immunomodulatory biomaterials and regenerative immunology: Future Science.

Wang, W., & Yeung, K. W. (2017). Bone grafts and biomaterials substitutes for bone defect repair: A review. *Bioactive Materials, 2*(4), 224-247.

Wang, Y., Qian, J., Zhao, N., Liu, T., Xu, W., & Suo, A. (2017). Novel hydroxyethyl chitosan/cellulose scaffolds with bubble-like porous structure for bone tissue engineering. *Carbohydrate Polymers, 167*, 44-51.

Wang, F., Wu, H., Venkataraman, V., & Hu, X. (2019). Silk fibroin-poly (lactic acid) biocomposites: Effect of protein-synthetic polymer interactions and miscibility on material properties and biological responses. *Materials Science and Engineering: C*, *104*, 109890.

White, T. D., & Folkens, P. A. (2005). *The human bone manual*: Elsevier.

Woodard, J. R., Hilldore, A. J., Lan, S. K., Park, C., Morgan, A. W., Eurell, J. A. C., . . . Johnson, A. J. W. (2007). The mechanical properties and osteoconductivity of hydroxyapatite bone scaffolds with multi-scale porosity. *Biomaterials, 28*(1), 45-54.

Wu, S., Liu, X., Yeung, K. W., Liu, C., & Yang, X. (2014). Biomimetic porous scaffolds for bone tissue engineering. *Materials Science and Engineering: R: Reports, 80*, 1-36.

Yang, S., Leong, K.-F., Du, Z., & Chua, C.-K. (2001). The design of scaffolds for use in tissue engineering. Part I. Traditional factors. *Tissue engineering, 7*(6), 679-689.

Yang, S., Leong, K. F., Du, Z., & Chua, C. K. (2001). The design of scaffolds for use in tissue engineering. Part I. Traditional factors. Tissue Engineering, 7(6), 679–689. https://doi.org/10.1089/107632701753337645

Yamamoto, S., Matsushima, Y., Kanayama, Y., Seki, A., Honda, H., Unuma, H., & Sakai, Y. (2017). Effect of the up-front heat treatment of gelatin particles dispersed in calcium phosphate cements on the in vivo material resorption and concomitant bone formation. *Journal of Materials Science: Materials in Medicine, 28*(3), 48.

Yang, F., Wolke, J. G. C., & Jansen, J. A. (2008). Biomimetic calcium phosphate coating on electrospun poly (ε-caprolactone) scaffolds for bone tissue engineering. *Chemical Engineering Journal*, *137*(1), 154-161

Yin, H.-M., Huang, Y.-F., Ren, Y., Wang, P., Zhao, B., Li, J.-H., . . . Li, Z.-M. (2018). Toward biomimetic porous poly (ε-caprolactone) scaffolds: Structural evolution and morphological control during solid phase extrusion. *Composites Science and Technology, 156*, 192-202.

Yildirim, N., & Shaler, S. (2017). A study on thermal and nanomechanical performance of cellulose nanomaterials (CNs). *Materials, 10*(7), 718.

Zare-Harofteh, A., Saber-Samandari, S., & Saber-Samandari, S. (2016). The effective role of akermanite on the apatite-forming ability of gelatin scaffold as a bone graft substitute. Ceramics International, 42(15), 17781-17791.

Zhao, X., Sun, X., Yildirimer, L., Lang, Q., Lin, Z. Y. W., Zheng, R., ... & Khademhosseini, A. (2017). Cell infiltrative hydrogel fibrous scaffolds for accelerated wound healing. Acta biomaterialia, 49, 66-77.

Zhang, C., Yuan, X., Wu, L., Han, Y., & Sheng, J. (2005). Study on morphology of electrospun poly (vinyl alcohol) mats. European polymer journal, 41(3), 423-432.

Zhang, C., Salick, M. R., Cordie, T. M., Ellingham, T., Dan, Y., & Turng, L. S. (2015). Incorporation of poly (ethylene glycol) grafted cellulose nanocrystals in poly (lactic acid) electrospun nanocomposite fibers as potential scaffolds for bone tissue engineering. Materials Science and Engineering: C, 49, 463-471.

Zhang, Z., & Michniak-Kohn, B. B. (2012). Tissue engineered human skin equivalents. *Pharmaceutics, 4*(1), 26-41.

Zhao, Y., He, M., Jin, H., Zhao, L., Du, Q., Deng, H., . . . Chen, Y. (2018). Construction of highly biocompatible hydroxyethyl cellulose/soy protein isolate composite sponges for tissue engineering. *Chemical Engineering Journal, 341*, 402-413.

Zhao, C., Tan, A., Pastorin, G., & Ho, H. K. (2013). Nanomaterial scaffolds for stem cell proliferation and differentiation in tissue engineering. *Biotechnology advances, 31*(5), 654-668.

Zheng, X., Hui, J., Li, H., Zhu, C., Hua, X., Ma, H., & Fan, D. (2017). Fabrication of novel biodegradable porous bone scaffolds based on amphiphilic hydroxyapatite nanorods. *Materials Science and Engineering: C, 75*, 699-705.

Zhou, C., Yang, K., Wang, K., Pei, X., Dong, Z., Hong, Y., & Zhang, X. (2016). Combination of fused deposition modeling and gas foaming technique to fabricated hierarchical macro/microporous polymer scaffolds. *Materials & Design, 109*, 415-424.
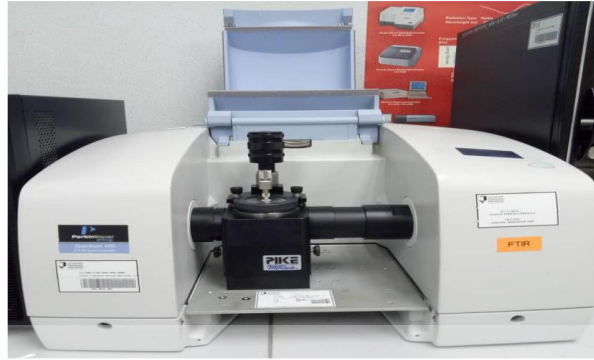
.

APPENDIX 1

INSTRUMENTS USED IN THIS STUDY

Scanning electron microscope (SEM)

Field emission scanning electron microscope

Attenuated total reflectance-Fourier transform infrared spectroscopy

Thermogravimetric components

Universal testing mechine (UTM)

APPENDIX 1I

PUBLICATION AND AWARDS

Etdal Bakhiet, S.F. Samsudin, F.H. Zulkifli, A.N.M. Ramli, Thermal Characterizations of HPMC/PVA Impregnated with CNC Electrospun Nanofibers, Materials Science Forum (2020) 981, 115 – 120.

Etdal Bakhiet, Nur Fatini Ilyana Mohamat Jauhari, F.H. Zulkifli, Biomineralization of hydrozyethyl cellulose/ sodium alginate for bone tissue, Materials Science Forum (2020) – Accepted.

OsteoCellulose: Novel substrate for bone tissue. Farah Hanani Zulkifli, Nor Sarahtul Nadirah Hairol Nizan, **Etdal Bakhiet**, Hazrulrizawati Hamid, Aizi Nor Mazila Ramli, Mohd Lokman Isa. International Invention, Innovation & Technology Exhibition (ITEX). 2020. – Gold Medal.

Bio-nanocomposite scaffolds by cellulose nanocrystal reinforcing modified cellulose as novel substrate for bone tissue engineering. Farah Hanani Zulkifli, Nor Sarahtul Nadirah Hairol Nizan, **Etdal Bakhiet**, Hazrulrizawati Hamid, Aizi Nor Mazila Ramli, Mohd Lokman Isa. Creation, Innovation, Technology & Research Exposition (CITREX). 2020.- Gold Medal.